

Title Page

Title: Sensitivity of water scarcity events to ENSO driven climate variability at the global scale

Submitted to: Hydrology and Earth System Sciences

Ted I.E. Veldkamp¹

Stephanie Eisner²

Yoshihide Wada^{3,4,5}

Jeroen C.J.H. Aerts¹

Philip J. Ward¹

¹ Institute for Environmental Studies (IVM), VU University Amsterdam, the Netherlands

² Center for Environmental Systems Research, University of Kassel, Kassel, Germany

³ Center for Climate Systems Research, Columbia University, New York, USA

⁴ NASA Goddard Institute for Space Studies, New York, USA

⁵ Department of Physical Geography, Utrecht University, Netherlands

Corresponding author:

Ted I.E. Veldkamp

Institute for Environmental Studies (IVM)

Faculty of Earth and Life Sciences

VU University Amsterdam

De Boelelaan 1087

1081 HB Amsterdam

The Netherlands

Email: ted.veldkamp@vu.nl

Tel: +31(0)205987521

Fax: +31(0)205989553

Acknowledgements & Author Contribution

T.I.E.V., J.C.J.H.A., and P.J.W. designed research; T.I.E.V., S.E. and Y.W. prepared datasets; T.I.E.V. analyzed data; and T.I.E.V., S.E., Y.W., J.C.J.H.A., and P.J.W. wrote the paper.

The research leading to this article is partly funded by the EU 7th Framework Programme through the projects ENHANCE (grant agreement no. 308438) and Earth2Observe (grant agreement no. 603608). J. Aerts received funding from the Netherlands Organisation for Scientific Research (NWO) VICI (grant no. 453-14-006). Y. Wada is supported by Japan Society for the Promotion of Science (JSPS) Oversea Research Fellowship (grant no. JSPS-2014-878). P. Ward received funding from the Netherlands Organisation for Scientific Research (NWO) in the form of a VENI grant (grant no. 863-11-011).

Abstract

Globally, freshwater shortage is one of the most important risks for society. Changing hydro-climatic and socioeconomic conditions have aggravated water scarcity over the past decades. A wide range of studies show that water scarcity will intensify in the future, as a result of both increased consumptive water use and, in some regions, climate change. Although it is well-known that ENSO affects patterns of precipitation and drought at global and regional scales, less attention has been paid yet to the impacts of climate variability on water scarcity conditions, despite its importance for adaptation planning. Therefore, we present the first global scale sensitivity assessment of water scarcity to El Niño-Southern Oscillation (ENSO), the most dominant signal of climate variability.

We show that over the time period 1961-2010, both water availability and water scarcity conditions are significantly correlated with ENSO driven climate variability over a large proportion of the global land-area ($>28.1\%$); an area inhabited by more than 31.4% of the global population. We also found, however, that climate variability alone is often not enough to trigger the actual incidence of water scarcity events. The sensitivity of a region to water scarcity events, expressed in terms of land-area or population exposed, is determined by both hydro-climatic and socioeconomic conditions. Currently, the population actually impacted by water scarcity events consists of 39.6% (CTA: Consumption to Availability ratio) and 41.1% (WCI: Water Crowding index) of the global population whilst only 11.4% (CTA) and 15.9% (WCI) of the global population is at the same time living in areas sensitive to ENSO driven climate variability. These results are contrasted however by differences in found growth rates under changing socioeconomic conditions, which are relatively high in regions exposed to water scarcity events.

Given the correlations found between ENSO and water availability and scarcity conditions, and the relative developments of water scarcity impacts under changing socioeconomic conditions, we suggest that there is potential for ENSO-based adaptation and risk reduction which could be facilitated by more research on this emerging topic.

Keywords

ENSO, climate variability, hydroclimatology, water scarcity, water resources availability, global hydrology

1. Introduction

Over the past decades, changing hydro-climatic and socioeconomic conditions have led to increased regional and global water scarcity problems (Alcamo et al., 1997; Kummu et al., 2010; van Beek et al., 2011; van Vliet et al., 2013; Veldkamp et al., 2015; Vörösmarty et al., 2000; Wada et al., 2011a). Freshwater shortage is recognized as one of the most important global risks, not only in terms of likelihood but also with respect to its impacts, with societal and economic consequences that result from the inability to meet water demands (Hanemann, 2006; Howell, 2013; Rijsberman, 2006; Young, 2005). In the near future, projected changes in human water use and population growth – in combination with climate change - are expected to aggravate water scarcity conditions and their associated impacts on society (Alcamo et al., 2007; Haddeland et al., 2014; Kiguchi et al., 2015; Lehner et al., 2006; Prudhomme et al., 2014; Schewe et al., 2014; Sperna Weiland et al., 2012; Stahl, 2001; van Vliet et al., 2013; Wada et al., 2014a).

Whilst a wide range of studies have assessed the role of long-term climate change and changing socioeconomic conditions on past and future global blue water availability and water scarcity events, the impact of inter-annual climate variability is less well understood (Kummu et al., 2014; Lundqvist & Falkenmark, 2010; Rijsberman, 2006; Veldkamp et al., 2015). Taking into account the impact of climate variability relative to longer-term changes in either the socioeconomic or climatic conditions is, however, important as these factors of change may amplify or offset each other at the regional scale (Hulme et al., 1999; McPhaden et al., 2006; Murphy et al., 2010; Veldkamp et al., 2015). Correct information on current and future water scarcity conditions and thorough knowledge on the relative contribution of its driving forces, such as inter-annual variability, help water managers and decisions makers in the design and prioritization of adaptation strategies for coping with water scarcity.

To address this issue, we assess in this paper the sensitivity of blue water resources availability (i.e. the water available in rivers and lakes), consumptive water use, and blue water scarcity events to climate variability driven by El Niño-Southern Oscillation (ENSO) at the global scale over the time period 1961-2010. Moreover, we evaluated whether those areas with a statistically significant correlations have been exposed to blue water scarcity events; if there is a spatial clustering in terms of population or land-area exposed to blue water scarcity events and/or population living in areas sensitive to ENSO driven climate variability, and whether this spatial clustering has changed over time given the socioeconomic developments. Within this contribution we investigate the impact of ENSO as it is the most dominant signal of inter-annual climate variability (McPhaden et al., 2006). Also, since ENSO can be predictable with reasonable skill up to several seasons in advance (Cheng et al., 2011; Ludescher et al., 2014), this can provide useful information for adaptation management to account for inter-annual variability in blue water resources and blue water scarcity estimates, enabling the prioritization of adaptation efforts in the most affected regions ahead of those extreme events (Bouma et al., 1997; Cheng et al., 2011; Dilley & Heyman, 1995; Ludescher et al., 2013; Ward et al., 2014a,b; Zebiak et al., 2014).

ENSO is the result of a coupled climate variability system in which ocean dynamics and sea level pressure interact with atmospheric convection and winds (ocean-atmosphere feedback mechanisms). El Niño is the oceanic

component, whereby waters over the eastern equatorial Pacific Ocean reach anomalously high temperatures. This eastern Pacific Ocean surface is relatively cool under neutral conditions, while it reaches anomalously low temperatures during La Niña conditions. The Southern Oscillation is the atmospheric component, represented by the east-west shifts in the tropical atmospheric circulation between the Indian and West Pacific Oceans and the East Pacific Ocean (Kiladis & Diaz, 1989; Parker et al., 2007; Rosenzweig & Hillel, 2008; Wallace & Hobbs, 2006; Wang et al., 2004). ENSO is well-known for its impacts on precipitation and hydrological extremes (such as drought and flooding) at local and regional scales (e.g. Chiew et al., 1998; Kiem & Franks, 2001; Lü et al., 2011; Mosley, 2000; Moss et al., 1994; Piechota & Dracup, 1999; Räsänen & Kumm, 2013; Whetton et al., 1990; Zhang et al., 2015). Several studies have also examined ENSO's impact at the global scale (Chiew & McMahon, 2002; Dai & Wigley, 2000; Dettinger et al., 2000; Dettinger & Diaz, 2000; Labat, 2010; Ropelewski & Halpert., 1987; Sheffield et al., 2008; Vicente-Serrano et al., 2011; Ward et al., 2010; Ward et al., 2014a). Though, only a limited number of studies assessed the societal impacts (e.g. in terms of population affected, GDP loss, or with respect to human health) of hydrological extremes under the different ENSO stages at the global scale (Bouma et al., 1997; Dilley & Heyman, 1995; Kovats et al., 2003; Rosenzweig & Hillel, 2008; Ward et al., 2014b). To the best of our knowledge, none of these studies have executed a global-scale assessment to the sensitivity of water scarcity events to ENSO driven climate variability, combining therein both the availability and consumptive demand for water resources as well as the exposure to adverse water scarce conditions.

2. Methods

2.1 Ensemble mean monthly runoff and discharge

We simulated global gridded daily discharge and runoff over the period 1960-2010 at a resolution of $0.5^\circ \times 0.5^\circ$ using three global hydrological models: PCR-GLOBWB (van Beek et al., 2011; Wada et al., 2014b), STREAM (Aerts et al., 1999; Ward et al., 2007) and WaterGAP (Müller Schmied et al., 2014), forced with WATCH Forcing Data - ERA Interim (WFDEI) daily precipitation and temperature data ($0.5^\circ \times 0.5^\circ$) (Weedon et al., 2014) for the period 1979-2010 and WATCH forcing data ERA40 (WFD) for the period 1960-1978 (Weedon et al., 2011). In order to compensate for offsets in long-term radiation fluxes between the two datasets, as found by Müller Schmied et al. (2014), WFD down-welling shortwave and longwave radiation were adjusted for use in WaterGAP to WFDEI long-term means following the approach of Haddeland et al. (2012). Daily values were aggregated to time-series of monthly discharge and runoff. Using global hydrological models gives us the advantage of a global coverage whereas the portfolio of observed datasets (water availability and consumptive water use) is bounded by its biased regional distribution (Hannah et al., 2011; Ward et al., 2010; Ward et al., 2014a). However, we are aware of the caveats using these types of models to estimate water availability as all large-scale hydrological models have their own strengths and shortcomings (Gudmundsson et al., 2012; Nazemi & Wheeler, 2015a, b). Therefore, we constructed ensemble-mean time-series of both monthly discharge and runoff capturing the three global hydrological models. The results of the individual modelling efforts were used to evaluate the modelling agreement (Section 2.4 and 3.5).

2.2 Calculating water availability

Water availability is expressed in this paper as the sum of monthly runoff per Food Producing Unit (FPU). FPU's represent a hybrid between river basins and economic regions for which it is generally assumed that water scarcity issues can be solved internally (Cai & Rosegrant, 2002; de Fraiture, 2007; Kummu et al., 2010; Rosegrant et al., 2002). We used here an updated version of the FPU's used by Kummu et al (2010), which consists of 436 FPU's, excluding small island FPU's. For FPU's located within one of the world's larger river basins we redistributed runoff in order to avoid local over- or under-estimations in water availability. Runoff was redistributed across the FPU's within these larger river basins, proportionally to the discharge distribution of that large river basin (Gerten et al., 2011; Schewe et al., 2014):

$$WA_i = \frac{R_b * Q_i}{\sum Q_i}, \quad \text{Eq. 1}$$

whereby WA_i is the monthly water availability within FPU i , R_b is the total monthly runoff within large river-basin b , Q_i is the monthly discharge in FPU i , and $\sum Q_i$ is the sum of the monthly discharge over all cells within large river-basin b .

Subsequently, we calculated the annual water availability by aggregating the simulated ensemble-mean monthly water availability time-series using hydrological years. The use of hydrological years is necessary in this assessment as ENSO tends to develop to its fullest strength during the period December – February, which intersects with the standard calendar year boundaries (Ward et al., 2014a, b). Hydrological years are referred to by the year in which they end, e.g. hydrological year 1961 refers here to the period October 1960 – September 1961. Within this study we follow Ward et al (2014a) and distinguish two hydrological years on the basis of long-term monthly maximum water availability per river basin: October – September (standard) and July – June (for river basins that have their long-term monthly maximum water availability in September, October or November). The river basin delineation used here was derived from the WATCH project (Döll & Lehner, 2002) and is equal to the river basin delineation that is used as the input for the FPU classification used within this study. We used the hydrological years setting determined at grid-level, using the WATCH river-basins, as input for the distinction between hydrological years at FPU scale. If an FPU consisted of more than one river basin we based the choice of hydrological year on the month (with long-term maximum water availability) with the highest prevalence within this FPU (see Fig. A.1).

2.3 Calculating consumptive water use

Monthly gridded water consumption ($0.5^\circ \times 0.5^\circ$) was estimated for the sectors livestock, irrigation, industry and domestic within PCR-GLOBWB using daily WFD-EI precipitation and temperature data in combination with yearly information on: livestock densities; the extent of irrigated areas; desalinated water use; non-renewable groundwater abstractions; and past socioeconomic developments, namely GDP, energy and electricity production, household consumption, and population growth (Wada et al., 2011b, 2014b). For a complete description and extensive discussion of the methodological steps taken to compose these monthly consumptive water use time-series, we refer to Wada et al. (2011b, 2014b). Time-series of desalinated water use and non-renewable ground water abstractions

were subtracted from the total consumptive water use estimates as they lower the need for blue water. Subsequently we aggregated gridded monthly consumptive water use into yearly totals per FPU ($WC_{i,yr}$), following the hydrological years. Since the resulting ‘transient’ consumptive water use estimates are partially driven by changing socioeconomic conditions (population, GDP, and growth in irrigated areas) and therefore disguise any possible correlations with ENSO driven climate variability, we repeated the steps above whilst we fixed the socioeconomic parameters at 1961 levels (following the hydrological year naming convention). These ‘fixed’ consumptive water use estimates were used to evaluate the sensitivity to ENSO driven climate variability (Section 3.1 and 3.2) whereas the ‘transient’ water consumption time-series were used to evaluate the development of water scarcity conditions under changing socioeconomic conditions (Section 3.3).

2.4 Calculating water scarcity conditions

Blue water scarcity refers to the imbalance between blue water availability (i.e. water in rivers, lakes and aquifers) and the needs for water over a specific time period and for a certain region (Falkenmark, 2013). Although water scarcity could also relate to the green (water in the unsaturated soil), white (part of rainfall that feeds directly back into the atmosphere), and deep blue (fossil ground water) water sources (Savenije, 2000), we focus here on blue water scarcity (hereafter: water scarcity) only. Within this study we applied two complementary indicators to express water scarcity conditions per FPU: the Water Crowding Index (WCI) for population-driven water shortage and the Consumption-to-Availability ratio (CTA-ratio) for demand-driven water stress (Brown & Matlock, 2011; Rijsberman, 2006). The WCI quantifies the yearly water availability per capita (Falkenmark, 1989, 2007, 2013), whereby water demands are based on household, agricultural, industrial, energy and environmental water consumption (Rijsberman, 2006). Like previous studies (e.g. Alcamo et al., 2007; Arnell, 2003; Kummu et al., 2010), we used 1700 m³/capita per year as the threshold level to evaluate water shortage events. The CTA-ratio evaluates the ratio between consumptive water used and water availability in a specific region and is a derivative from the Withdrawal-to-Availability (Raskin et al., 1997). Usually, a region is said to experience water stress events when water withdrawals comprises $\geq 40\%$ of the available water resources, whilst moderate water stress conditions occur if $20\% \geq WTA \leq 40\%$ (Raskin et al., 1997). These values are widely quoted and applied in previous research contributions, e.g. by Alcamo et al. (2003, 2007), Arnell et al. (1999), Cosgrove & Rijsberman (2000), Hanasaki et al. (2013), Kiguchi et al. (2015), Kundzewich et al. (2007), Oki et al. (2001, 2006), Vörösmarty et al. (2000). Hoekstra et al. (2012) and Wada et al. (2011a) applied this WTA-ratio in an adapted form, using blue water footprints and potential consumptive water use estimates respectively to assess water stress conditions: the CTA-ratio. This approach accounts for the share of water that has been recycled (industry) or not used (irrigation) and which flows back into the natural system. The threshold level for water stress using these consumptive water demands is therefore conceived to be lower than the threshold level for water stress as estimated using withdrawals. Following Hoekstra (2011, 2012), Richter et al. (2012), and Wada et al. (2011a), we applied a threshold level of 0.2 to indicate water stress events. Equations 2 and 3 show the use of the WCI ($WCI_{i,yr}$) and the CTA-ratio ($CTA_{i,yr}$), respectively:

$$WCI_{i,yr} = \frac{WA_{i,yr}}{P_{i,yr}} \quad (\text{water shortage event if } WCI_{i,yr} \leq 1700) , \quad \text{Eq. 2}$$

$$CTA_{i,yr} = \frac{WC_{i,yr}}{WA_{i,yr}} \quad (\text{water stress event if } CTA_{i,yr} \geq 0.2) , \quad \text{Eq. 3}$$

whereby $WA_{i,yr}$ is the water available per spatial unit i and hydrological year yr , $P_{i,yr}$ is the population, and $WC_{i,yr}$ is consumptive water use. Water scarcity conditions were assessed here at the FPU-scale. The FPU scale is seen as an appropriate spatial scale to study water scarcity conditions as it is generally assumed that lower-scale water scarcity issues can be overcome by the reallocation of water demand and supply within this spatial unit (Kummu et al., 2010). However, one should keep in mind that, due to the assumption of full exchange possibilities –both from an infrastructural and water management perspective– and its relative large spatial scale, analysis executed at the FPU-scale may disguise lower-scale water scarcity issues (Kummu et al., 2010; Wada et al., 2011a).

The population data used for the calculation of the WCI (Eq. 2) were adopted from Wada et al. (2011a, b), who derived yearly gridded population maps ($0.5^\circ \times 0.5^\circ$) from yearly country-scale FAOSTAT data in combination with decadal gridded global population maps (Klein Goldewijk & van Drecht, 2006). We aggregated these gridded population maps to FPU-scale for use in this study. In line with the hydrological year naming convention, population estimates were used for the year in which the hydrological year ends, e.g. for hydrological year 1961 we used population estimates of 1961 as input for the WCI and to calculate water scarcity impacts.

2.5 Sensitivity of water availability, consumptive water use, and water scarcity conditions to ENSO

We examined the relationship respectively between water availability, consumptive water use, and water scarcity conditions, and ENSO driven climate variability by means of their correlation with the Japan Meteorological Agency's (JMA) Sea Surface Temperature (SST) anomaly index (<http://coaps.fsu.edu/jma.html>). We used here three-monthly mean values of the JMA SST over the periods October-December, November-January, December-February, and January-March, as El Niño and La Niña expressions are strongest in these months (Dettinger & Diaz, 2000). Following Ward et al. (2014b), we examined the correlation between WA_{ann} , WC_{ann} , CTA_{ann} , and WCI_{ann} , and the 3-monthly mean JMA SST values (OND, NDJ, DJF, JFM), using Spearman's rank correlation coefficient. Statistical significance was assessed by means of regular bootstrapping ($n = 1000$, $p \leq 0.05$) while field significance, i.e. the joint statistical significance of multiple individual significance tests (Livezey & Chen, 1982; Wilks, 2006), for each of the 3-monthly JMA SST correlation values was tested using the binomial distribution (Livezey & Chen, 1982). With field significance testing we counted the number of individual tests with a significant result and assessed the probability of yielding this result by chance given its statistical distribution (Livezey & Chen, 1982; Wilks, 2006). Subsequently, we examined the percentage anomalies in the median values of water scarcity conditions between El Niño (EN) and La Niña (LN) years, compared to the median values under all years. To distinguish between El Niño, La Niña and neutral years we used the classification of ENSO years from the Center for Ocean-Atmospheric Prediction Studies based on the JMA SST values. Years are assigned as El Niño or La Niña years when their 5-month moving average JMA SST index values are $(\pm)0.5^\circ\text{C}$ or greater (El Niño)/ smaller (La

Niña) for at least six consecutive months (including October-December). Reference to the different ENSO years was adjusted to be consistent with the naming convention used for the hydrological years (Table 1). We used a bootstrapped version of the non-parametric Mann-Whitney U test ($n = 1000$, $p \leq 0.05$) to test the statistical differences in median values.

[Table 1 approximately here]

The critical threshold-values put in place for the WCI and the CTA-ratio (here: 1700 and 0.2 respectively) determine whether water scarcity conditions adversely affect population or society. Per FPU we therefore evaluated which proportion of land-area, for which we found a significant correlation between ENSO and water scarcity conditions, is also exposed to water scarcity events and how population is clustered in these areas compared to the general pattern of population density. Moreover we assessed how these numbers changed through time given the changing socioeconomic conditions, relative to developments in: (1) the population and land-area sensitive to ENSO driven climate variability but not exposed to water scarcity events; (2) the population and land-area exposed to water scarcity events, in areas that lack a significant correlation with ENSO driven climate variability; and to (3) the total population growth.

2.6 Evaluating modelling uncertainty

A cross-model validation was executed in order to evaluate the modelling uncertainty whereby we compared the results from the ensemble-mean with the outcomes of the individual global hydrological models. We examined the agreement among the different modelling results and the ensemble-mean when looking at: (1) the sensitivity of water availability and water scarcity conditions to ENSO driven climate variability; and (2) the impacts of water scarcity events and relation to ENSO driven climate variability under changing socioeconomic conditions.

3 Results

3.1 Sensitivity of water availability and consumptive water use to ENSO

Significant correlations of water availability to variations in JMA SST were found across 37.1% of the global land surface (excluding Greenland and Antarctica) whilst we found for consumptive water use (simulated under fixed socioeconomic conditions at 1961 levels), significantly correlations covering 8.3% of the total land area (Fig. 1 and Table 2). Using the 3-monthly JMA SST period with the highest correlation, Fig. 1 shows for both water availability and consumptive water use its correlation coefficient with the inter-annual variation in the 3-monthly average JMA SST values. Only those correlations which reach statistical significance at a 95% confidence interval are shown here. Field significance, the collective ‘global’ significance of the total of individual ‘local’ hypothesis tests (Livezey & Chen, 1982; Wilks, 2006), was tested for the individual 3-month correlation results and found to be highly significant when looking at water availability ($p < 0.01$) but insignificant when considering consumptive water use ($p > 0.5$). Positive correlations, i.e. more water available with the JMA SST index moving towards El Niño values, were found for 13.2% of the global land surface, while negative correlations were found in FPU

covering 23.9% of the global land surface. When looking at consumptive water use we found positive significant correlations for only 1.0%, and negative correlations for 7.3% of the global land surface.

[Figure 1 approximately here]

[Table 2 approximately here]

3. 2 Sensitivity of water scarcity conditions to ENSO

Subsequently, we assessed how sensitive water scarcity conditions (simulated under fixed socioeconomic conditions at 1961 levels) are to ENSO driven climate variability. Significant correlations to variations in JMA SST were found for 28.1% and 37.9% of the global land surface when using the CTA-ratio (water stress) and WCI (water shortage) respectively, while being tested under a 95% confidence interval (Table 3). Due to the clustering of population and consumptive water use we found even higher percentages when looking at the population living in these areas, 31.4% and 38.7% of the global population in 2010 for the CTA-ratio and WCI respectively.

[Table 3 approximately here]

Fig. 2 shows the areas with a significant positive (red) or negative (blue) correlation of water stress conditions (CTA-ratio) with the variation in JMA SST values, using the 3-monthly JMA SST period with the highest correlation (JMA SST_{bestoff}). Correlation results found for water shortage conditions, as defined by the WCI, show a similar pattern as for water stress and are given in Fig. A.2. For both metrics, we found that, for a majority of the land-area with a significant correlation to ENSO driven climate variability, water scarcity conditions become more severe when the JMA SST index moves towards El Niño values (Table 3).

[Figure 2 approximately here]

The regional variation in sensitivity of water scarcity conditions to ENSO driven variability (Fig. 2 and Fig. A.2) is clearly driven by the spatial distribution of water availability correlations as the general patterns are similar to those found in Fig. 1. The unequal clustering of water availability and consumptive water use leads, however, in some regions to a strengthening or weakening of the correlation signal, for example when comparing the regional variation in sensitivity results for water stress within the Amazon basin or in Southern Africa (Fig. 2) with the regional variation in correlation results for water availability in those areas (Fig. 1). For a selection of FPU, we found significant correlations for both water availability and consumptive water use, while they lack significant correlations when considering water stress conditions, and vice versa. In Southeast Asia, for example, we observed significant correlations between ENSO and water availability and consumptive water use (Fig. 1), but no significant correlations between ENSO and water stress (Fig 2). One explanation for this observation could be that if both water availability and consumptive water use increase or decrease with more or less the same strength under changing

JMA SST values, the net effect on the CTA-ratio could be insignificant since the ratio between both variables remains equal. All FPU's that show a significant correlation between water resources availability and ENSO driven climate variability show as well a significant correlation with ENSO driven variability when looking at the water shortage conditions (Fig. A.2). This can be explained by the fact that the WCI is only driven by changes in water availability and population growth, of which the latter factor was fixed in this analysis.

Subsequently, we assessed the percentage anomalies in the median values of water scarcity conditions between El Niño (EN) and La Niña (LN) years, compared to the median values under all years. Significant anomalies ($p \leq 0.05$, tested by regular bootstrapping $n = 1000$) in water scarcity conditions under El Niño and La Niña years, compared to all years, were found for 12.8% and 14.8% of the global land-area using the CTA-ratio and the WCI respectively (Table 4). Strongest signals anomaly signals were found during the La Niña phase for both water stress and shortage conditions.

[Table 4 approximately here]

Not all regions with a significant anomaly under El Niño years show (significant) anomalies in the opposite direction during La Niña years. For example, Fig. 3 visualizes the asymmetry in the anomalies found during the El Niño and La Niña phase for Latin America. Moreover, areas with significant correlations with the JMA SST index do not always show significant anomalies when looking at the different ENSO phases. This can be explained by the fact that only those years for which the 5-month moving average JMA SST index values are ≥ 0.5 °C or greater (El Niño)/ smaller (La Niña) for at least six consecutive months (including October-December) are assigned as El Niño or La Niña years (see Section 2.5). Using this ENSO year definition thus disguises all variability in JMA SST values that falls just below the threshold set, variation that can have a significant effect on water scarcity conditions however.

[Figure 3 approximately here]

3.3 Sensitivity of water scarcity events to ENSO under changing socioeconomic conditions

Due to the socioeconomic developments over the period 1961-2010 water scarcity conditions and their associated impacts intensified, both in absolute and relative sense (Fig. 4 and Table 5). From 1961 to 2010, using 5-year averaged values, the total global population increased from 2.97 to 6.25 billion. At the same time, we found that the global population exposed to water scarcity events increased from 0.45 billion to 2.47 billion. The global population sensitive to ENSO driven climate variability increased with a factor 2.4 over the same time period whilst its proportion to the global total population remained rather unchanged (Table 5). The population sensitive to ENSO variability and living in areas exposed to water scarcity events currently represent only a minority of the global population (11.4%). These results are, however, contrasted with relative high growth factors (Table 5). The impact the spatial clustering of population and consumptive water use, and their unequal growth rates, on water scarcity events is shown by the fact that the share of land-area exposed to water scarcity events only doubled over this same

period for the CTA-ratio (Fig. 4), from 7.4% up to 16.5% of the global land surface . The results found under for water shortage ($WCI \leq 1700$) are roughly similar at the global scale (Fig. A.3, Table A.1) and therefore not discussed individually in this section.

[Figure 4 approximately here]

[Table 5 approximately here]

Regional variations in the population exposed to water stress and/or being sensitive to ENSO driven climate variability under changing socioeconomic conditions, are visualized in Fig. 5. Although these regional figures do not lend themselves to a similar growth factor analysis such as executed on the global numbers in Fig. 4, we can distinguish by means of visual inspection different characteristic region-types. The first group of regions (Latin America Australia & the Pacific, the Caribbean, and Middle & Southern Africa) experiences significant correlations with ENSO variability for a relative large share of its land-area and population ($\geq 25\%$ of the total population in 2010) whilst exposure to water scarcity events is low ($< 25\%$ of the total population in 2010). The second group of regions shows both a relatively low sensitivity to ENSO driven climate variability ($< 25\%$ of the total population in 2010) and low exposure to water scarcity events ($< 25\%$ of the total population in 2010), e.g. Northern America and Western Europe. For the third group of regions (the Middle East, India, Southeast Asia, and West & Central Asia) we find significant water scarcity exposure ($\geq 25\%$ of the total population in 2010) but no or relative low sensitivity to ENSO variability ($< 25\%$ of the total population in 2010). Finally, the fourth group of regions shows relatively high exposure to water scarcity events ($\geq 25\%$ of the total population in 2010) and abundant sensitivity to ENSO driven climate variability ($\geq 25\%$ of the total population in 2010), e.g. China and Northern Africa. Comparing these observations with the regional figures found for water shortage events (Fig. A.4), assessed by means of the WCI, we found different results for the regions West & Central Asia (relative high sensitivity to ENSO variability & relative low water scarcity exposure), and Middle & Southern Africa, the Middle East and Southeast Asia (both experiencing relative high sensitivity to ENSO variability & high exposure to water scarcity events). Using both water scarcity metrics (i.e. CTA-ratio and WCI) in combination with the observed growth rates in population and population exposed to water scarcity events enables us to identify those regions where adaptation measures such as ENSO-based forecasting have the largest (future) potential in coping with and possibly reducing the adverse impacts of water scarcity events: the Caribbean, Latin America, Western & Central Asia, Middle & Southern Africa, Northern Africa, the Middle East, China, Southeast Asia and Australia & the Pacific.

[Figure 5 approximately here]

3.4 Cross-model validation

The cross-model validation exercise, in which we compared the outcomes of the individual global hydrological models with their ensemble mean results, reveals that our findings considering the sensitivity of water availability,

consumptive water use, and water scarcity conditions to ENSO driven climate variability are robust to the use of different hydrological models. We found that for 22.8% of the global land-area (61.4% of the total land area with a significant correlation under the ensemble-mean) all individual GHMs show a significant correlation to variations in JMA SST in the same direction as the correlation results found under the ensemble-means. Correlations found under the ensemble-mean are supported by at least one global hydrological models for one-third (36.8%) of the global land surface (Fig. 6), equal to 99.2% of the land area that shows a significant correlation to the ensemble-mean.

[Figure 6 approximately here]

A comparison of the individual modelling results with the ensemble-mean in terms of the estimated population exposed to water scarcity events and/or living in areas sensitivity to ENSO driven climate variability shows the modelling spread at the global scale with respect to estimated impacts and their developments over time (Fig. 7). Looking at the 2010 values, we find the smallest percentage difference between models in the estimates of the population exposed to water scarcity events (+17.2% CTA-ratio, +21.8% WCI), and the largest variations when looking at the population both being exposed to water scarcity events and living in areas sensitive to ENSO driven climate variability (+68.9% CTA-ratio, +54.2% WCI). Percentage deviations were found to be smaller when looking at the land-area exposed (Fig. A.10). As shown in Fig. 7 and Fig. A.5, the inter-model comparison reveals that the impact estimates of the ensemble-mean are conservative when comparing them with the individual modelling results, especially when looking at the population or land-area sensitive to ENSO variability and/or being exposed to water scarcity events.

[Figure 7 approximately here]

4. Discussion

Within this study we found that both water resources availability and water scarcity conditions can be significantly correlated with ENSO driven climate variability as measured with the JMA SST index for a relative large share of the global land-area. Due to clustering effects we found even larger proportions when looking at the population living in these areas.

Regions well-known for their correlation of precipitation and hydrological extremes with ENSO variability (Dai & Wigley, 2000; Dettinger and Diaz, 2000; Ropelewski & Halpert., 1987; Vicente-Serrano et al., 2011; Ward et al., 2010, 2014a) also showed a statistically significant correlation between ENSO and annual total water resources availability or water scarcity conditions. This makes sense as precipitation deficits feed droughts, which possibly results in water scarcity events if consumptive demands outweigh the available water resources. On the other hand precipitation surpluses might result in increased water levels, floods, and increased flood risk but at the same time decreased water scarcity conditions. When comparing our results on water resources availability to these previous studies, we find corresponding significant correlations in the regions mid-west North-America, the Caribbean, Latin

America, Southern Africa, South-East and Central Asia and the Pacific. Moreover, the sign of the correlations found within four large river basins in Latin America and Africa, (Amazon Congo, Paraná, and Nile) is supported by earlier estimates of Amarasekera et al. (1997) who assessed the correlation between ENSO and the natural variability in the flow of tropical rivers. Significant correlations as shown for other regions were also found in case studies focusing on Northern America (e.g. Clark II et al., 2014; Schmidt et al., 2001), South-east Asia (e.g. Lü et al., 2011; Räsänen & Kummu, 2013), Southern Africa (e.g. Meque & Abiodun, 2014; Richard et al., 2001), and Australia (e.g. Chiew et al., 2011; Dutta et al., 2006). The spatial variation in sign of the found correlation is in line with the results of Ward et al. (2014a), who found that annual flood and mean discharge values intensify under La Niña and decline when moving towards El Niño phases globally in more areas than the other way around.

In line with earlier research (e.g. Meza et al., 2005; Islam & Gan, 2015) we would have expected to find more areas with a significant correlation between consumptive water use and ENSO driven climate variability. A number of explanations could be given for the absence of significant correlations patterns in this study: 1) the consumptive water use estimates used in this study are calculated by means of multiple socioeconomic and hydro-climatic proxies and variables, such as extent of irrigated areas, number of livestock, GDP, (long-term mean) monthly temperatures, and precipitation estimates, and should be interpreted as potential consumptive water use; 2) of these variables only irrigation water use could be linked directly to ENSO driven climate variability by means of its temperature and precipitation input variables. 'Fixed' consumption numbers in other sectors might attenuate therefore the variability found within the irrigation sector; 3) climate-driven variations in irrigation water demands are the result of changes in crop evapotranspiration and changes in green water availability, which do not have a univocal relation with ENSO driven climate variability at all times, but are partly determined by the month-specific cropping calendar and antecedent conditions, such as the memory of the soil (i.e. the ability of the soil to 'remember' anomalous wet or dry conditions long after these conditions occurred in the atmosphere or any other stage of the hydrological cycle (Seneviratne et al., 2006); and 4) yearly totals of consumptive water use were applied in this study to assess its sensitivity to ENSO driven climate variability whereas it might be more appropriate for consumptive water use to assess its correlation either using monthly time-scales or yearly maxima.

The analysis presented in this study revealed that inter-annual variability itself, such as the ENSO driven climate variability, is often not enough to cause water scarcity events to actually occur. We found that it is a combination of multiple hydro-climatic factors, such as the mean water resources availability and its inter-annual variability around the mean, together with the prevalent socioeconomic conditions, that determines the susceptibility of a region to water scarcity events, a finding earlier suggested by Veldkamp et al. (2015) and Wada et al. (2011a), and its implications being discussed in Hall & Borgomeo (2013). The actual impact of water scarcity events depends, moreover, not only on the number of people exposed or the severity of a water scarcity event itself, but on how sensitive this population is to water scarcity conditions, whether and how efficiently governments can deal with water scarcity problems, and how many (financial and infrastructural) resources are available to cope with these water scarce conditions (Grey & Sadoff, 2007; Hall & Borgomeo, 2013).

Given the substantial share of land-area, and the even higher rates of population, for which water resources availability and water scarcity conditions show significant correlations with ENSO driven climate variability there is a large potential for ENSO based adaptation and risk reduction to cope with water scarcity events and their associated impacts. The relative importance of ENSO driven climate variability in the year-to-year-variability as found in this study could assist water managers and decisions makers in the design of adaptation strategies, such as in optimizing the use of existing reservoir facilities in Australia (Sharma, 2000). Moreover, the potential predictability of ENSO with lead times up to several months, may help in the prioritization of (ex-ante) efforts in disaster risk reduction, such as pre-stocking foods and disaster relief goods or crop insurance systems based on ENSO indices (Coughlan de Perez et al., 2014, 2015; Dilley, 2000; Suarez et al., 2008). Potential added value of adaptation measures targeting on the impacts of inter-annual variability is high, as it is especially this variability that people find difficult to cope with (Smit & Pilifosova, 2003). In this paper we looked, however, at naturalized flows, no reservoirs or inter-basin transfers were taken into account yet. Future research should therefore, first evaluate whether (virtual) water trading and water storage mechanisms are effective in reducing water scarcity conditions and whether management could be optimized using ENSO-forecasting parameters and at what costs.

To get more insight in the expected correlation between ENSO, and water resources and scarcity conditions under longer-term climate change and socioeconomic developments, future research could use extreme JMA SST values as a test case in combination with the correlation values found to extrapolate the water resources and scarcity conditions under extreme events. Recent research showed that these extreme ENSO events may become more recurrent in the future (Cai et al., 2014; IPCC, 2013; Power et al., 2013). The uncertainty among the different climate models is, however, large and at the same time there is no agreement yet on the attribution of long-term climate change to increases in the sensitivity and frequency of ENSO events (Van Oldenborgh et al., 2005; Paeth et al., 2008; Guilyardi et al. 2009). Considering a continuous increase in population growth and water scarcity impacts in the future, hotspots could be appointed that have to deal with water scarcity events and are sensitive to ENSO driven variability at the same time. One should take into account, however, that we assumed in this study that the found correlations between water availability, consumptive water use, and water scarcity conditions, and the JMA SST index value remain stationary over time. In reality, the strength of correlations between hydrological parameters and ENSO can change over time (Ward et al., 2014a). Further research is therefore needed to assess whether, how much, and in which direction these observed correlation values change under the combination of changing climatic conditions and historic and future socioeconomic developments. Moreover, ENSO is part of an ocean-atmospheric climate variability system that constitutes of many more sub-regional systems and local circulation patterns (e.g. Indian Monsoon and European weather systems) which modulate the ENSO signal. Future research should look into the sensitivity of water resources availability and scarcity conditions to combinations of these systems.

Global assessment studies, such as the one presented here, are well able to identify the impact of ENSO on global-scale patterns of water scarcity. These types of studies are therefore well-suited for a first-order problem definition or for the large-scale prioritization of adaptation efforts. When interpreting these assessments one should keep in

mind, however, that these studies should always be complemented with local or regional scale analyses to assess the actual level of water scarcity ‘on the ground’, their (economic) consequences, and regional or local scale potential for ENSO forecasting as adaptation strategy to cope with water scarcity events.

5. Conclusions

Within this contribution, we executed the first global-scale sensitivity assessment of blue water availability, consumptive water use, and water scarcity to ENSO driven climate variability. Throughout this paper we have shown that regional water scarcity conditions become more extreme under El Niño and La Niña phases covering a relative large proportion (>28.1%) of the global land-area. Due to the spatial clustering of population and consumptive water use we found even larger shares (>31.4% of the total population in 2010) when looking at the population living in these areas being sensitive to ENSO driven climate variability. The exposure of a region to water scarcity events is determined by both hydro-climatic and socioeconomic conditions. Results on exposure to water scarcity events, found in this study, provide mixed signals. We found that the population that is currently exposed to water scarcity events consists of less than half of the global population (CTA-ratio: 39.6%, WCI: 41.1%), whilst the population sensitive to ENSO variability and living in areas exposed to water scarcity events represent only a minority of the global population (CTA-ratio: 11.4%, WCI: 15.9%). These results are, however, contrasted by relative differences in growth rates under changing socioeconomic conditions, which are higher in regions exposed to water scarcity events than in regions that do not experience any water scarcity.

Given the correlations found in this study for water availability and water scarcity conditions with ENSO driven climate variability, and seen the developments in the population and land-area exposed to water scarcity events and/or being sensitive to ENSO driven variability under changing socioeconomic conditions, we found that there is large potential for ENSO based adaptation and risk reduction. The observed regional variations could thereby accommodate in a first-cut prioritization for such adaptation strategies. Moreover, the results presented in this study show that there is both potential and need for more research on the issue of ENSO and water scarcity with emerging topics related to the economic impacts of water scarcity; the assessment of consumptive water use and its temporal variability; the combined impact of large scale oscillation systems on water resources and water scarcity conditions; and the transferability of global scale insights to local-scale implications and decisions.

References

- Aerts, J. C. J. H., Kriek, M., & Schepel, M. (1999). STREAM (Spatial Tools for River Basins and Environment and Analysis of Management Options): "Set Up and Requirements." *Phys. Chem. Earth (B)*, 24(6), 591–595.
- Alcamo, J., Döll, P., Kaspar, F., & Siebert, S. (1997). Global change and global scenarios of water use and availability: An Application of WaterGAP1.0 (p. 47). University of Kassel, Germany.
- Alcamo, J., Döll, P., Henrichs, T., Kaspar, F., Lehner, B., Rösch, T., Siebert, S. (2003). Global estimates of water withdrawals and availability under current and future 'business-as-usual' conditions. *Hydrological Sciences Journal*, 48 (3), 339–348. doi:10.1623/hysj.48.3.339.45278.
- Alcamo, J., Flörke, M., & Märker, M. (2007). Future long-term changes in global water resources driven by socioeconomic and climatic changes. *Hydrological Sciences Journal*, 52(2), 247–275. doi:10.1623/hysj.52.2.247
- Amarasekera, K. N., Lee, R. F., Williams, E. R., & Eltahir, E. A. B. (1997). ENSO and the natural variability in the flow of tropical rivers, *Journal of Hydrology*, 200, 24–39. doi:10.1016/S0022-1694(96)03340-9
- Arnell, N.W. (1999). Climate change and global water resources. *Environmental Change*, 9, S31–S49.
- Arnell, N. W. (2003). Effects of IPCC SRES* emissions scenarios on river runoff: a global perspective. *Hydrology and Earth System Sciences*, 7(5), 619–641. doi:0.5194/hess-7-619-2003
- Bouma, M. J., Kovats, R. S., Goubet, S. A., Cox, J. S. H., & Haines, A. T. (1997). Global assessment of El Niño 's disaster burden. *The Lancet*, 350, 1435–1438.
- Brown, A., & Matlock, M. D. (2011). A review of water scarcity indices and methodologies. *The Sustainability Consortium*, White paper, 106, 19.
- Cai, W., Borlace, S., Lengaigne, M., van Rensch, P., Collins, M., Vecchi, G., Timmermann, A., Santoso, A., McPhaden, M.J., Wu, L., England, M.H., Wang, G., Guilyardi, E., & Jin, F.-F. (2014). Increasing frequency of extreme El Niño events due to greenhouse warming. *Nature Climate Change*, 4(2), 111–116. doi:10.1038/nclimate2100
- Cai, X. M., & Rosegrant, M. W. (2002). Global Water Demand and Supply Projections. *Water International*, 27(2), 159–169. doi:10.1080/02508060208686989
- Cheng, Y., Tang, Y., & Chen, D. (2011). Relationship between predictability and forecast skill of ENSO on various time scales. *Journal of Geophysical Research*, 116(C12), C12006. doi:10.1029/2011JC007249
- Chiew, F. H. S., Piechota, T. C., Dracup, J. A., & McMahon, T. A. (1998). El Nino Southern Oscillation and Australian rainfall, streamflow and drought: Links and potential for forecasting. *Journal of Hydrology*, 204(1-4), 138–149. doi:10.1016/S0022-1694(97)00121-2
- Chiew, F. H. S., & McMahon, T. A. (2002). Global ENSO-streamflow teleconnection, streamflow forecasting and interannual variability. *Hydrological Sciences Journal*, 47(3), 505–522. doi:10.1080/02626660209492950
- Chiew, F. H. S., Young, W. J., Cai, W., & Teng, J. (2011). Current drought and future hydroclimate projections in southeast Australia and implications for water resources management. *Stochastic Environmental Research and Risk Assessment*, 25(4), 601–612. doi:10.1007/s00477-010-0424-x

574 Clark II, C., Nnaji, G. A., & Huang, W. (2014). Effects of f El-Niño and a La-Niña Sea Surface Temperature
575 Anomalies on Annual Precipitations and Streamflow Discharges in Southeastern United States. *Journal of*
576 *Coastal Research*, 68, 113–120. doi:10.2112/SI68-015.1

577 Cosgrove, W. & Rijsberman, F. (2000). *World water vision: Making water everybody's business*, Earthscan:
578 London.

579 Coughlan de Perez, E., Monasso, F., van Aalst, M., & Suarez, P. (2014). Science to prevent disasters. *Nature*
580 *Geoscience*, 7(2), 78–79. doi:10.1038/ngeo2081

581 Coughlan de Perez, E., van den Hurk, B., van Aalst, M., Jongman, B., Klose, T., & Suarez, P. (2015). Forecast-
582 based financing: an approach for catalyzing humanitarian action based on extreme weather and climate
583 forecasts. *Natural Hazards and Earth System Sciences*, 15, 895-904. doi:10.5194/nhess-15-895-2015

584 Dai, A., & Wigley, T.M.L. (2000). Global patterns of ENSO-induced precipitation *Geophysical Research Letters*,
585 27 (9), 1283-1986. Doi: 10.1029/1999GL011140.

586 De Fraiture, C. (2007). Integrated water and food analysis at the global and basin level. An application of
587 WATERSIM. *Water Resources Management*, 21, 185–198. doi:10.1007/s11269-006-9048-9

588 Dettinger, M. D., Cayan, D. R., McCabe, G. J., & Marengo, J. A. (2000). Multiscale streamflow variability
589 associated with El Niño / Southern Oscillation. In *El Nino and the Southern Oscillation - Multiscale*
590 *Variability and Global and Regional Impacts* (pp. 113–146), Cambridge University Press.

591 Dettinger, M. D., & Diaz, H. F. (2000). Global Characteristics of Stream Flow Seasonality and Variability. *Journal*
592 *of Hydrometeorology*, 1, 289–310.

593 Dilley, M., & Heyman, B. N. (1995). ENSO and Disaster: Droughts , Floods and El Nino/Southern Oscillation
594 warm Events. *Disasters*, 19(3), 181–193.

595 Dilley, M. (2000). Reducing vulnerability to climate variability in Southern Africa: The growing role of climate
596 information. *Climatic Change*, 45(1), 63–73.

597 Döll, P., & Lehner, B. (2002) Validation of a new global 30-min drainage direction map. *Journal of Hydrology*, 258
598 (1-4), 214-231. doi:10.1016/S0022-1694(01)00565-0

599 Dutta, S. C., Ritchie, J. W., Freebairn, D. M., & Abawi, G. Y. (2006). Rainfall and streamflow response to El Niño
600 Southern Oscillation: a case study in a semiarid catchment, Australia. *Hydrological Sciences Journal*, 51(6),
601 1006–1020. doi:10.1623/hysj.51.6.1006

602 Falkenmark, M., Jundqvist, L., & Widstrand, C. (1989). Macro-scale water scarcity requires micro-scale
603 approaches: aspects of vulnerability in semi-arid development. *Natural Resources Forum*, 13, 258–
604 267. doi:10.1111/j.1477-8947.1989.tb00348.x

605 Falkenmark, M., Berntell, A., Jagerskog, A., Lundqvist, J., Matz, M., Tropp, H. (2007). On the Verge of a New
606 Water Scarcity: A Call for Good Governance and Human Ingenuity. *Stockholm International Water Institute*
607 (SIWI).

608 Falkenmark, M. (2013). Growing water scarcity in agriculture : future challenge to global water security.
609 *Philosophical Transactions of the Royal Society A: Mathematical, Physical and Engineering Sciences*,
610 371(20120410). Doi: <http://dx.doi.org/10.1098/rsta.2012.0410>

611 Gerten, D., Heinke, J., Hoff, H., Biemans, H., Fader, M., & Waha, K. (2011). Global Water Availability and
612 Requirements for Future Food Production. *Journal of Hydrometeorology*, 12, 885–899.
613 doi:10.1175/2011JHM1328.1

614 Guilyardi E., Wittenberg, A., Fedorov, A., Collins, M., Wang, C., Capotondi, A., van Oldenborgh, G.J., &
615 Stockdale, T. (2009). Understanding El Niño in ocean–atmosphere general circulation models. Progress and
616 challenges. *Bull Am Meteorol Soc*, 90:325–340. doi: 10.1175/2008BAMS2387.1

617 Grey, D., & Sadoff, C. W. (2007). Sink or Swim? Water security for growth and development. *Water Policy*, 9(6),
618 545. doi:10.2166/wp.2007.021

619 Gudmundsson, L., Wagener, T., Tallaksen, L. M., & Engeland, K. (2012). Evaluation of nine large-scale
620 hydrological models with respect to the seasonal runoff climatology in Europe. *Water Resources Research*,
621 48(11), n/a–n/a. doi:10.1029/2011WR010911

622 Haddeland, I., Heinke, J., Voß, F., Eisner, S., Chen, C., Hagemann, S., & Ludwig, F. (2012). Effects of climate
623 model radiation, humidity and wind estimates on hydrological simulations. *Hydrol. Earth Syst. Sci.*, 16, 305–
624 318, doi:10.5194/hess-16-305-2012

625 Haddeland, I., Heinke, J., Biemans, H., Eisner, S., Flörke, M., Hanasaki, N., Konzmann, M., Ludwig, F., Masaki,
626 Y., Schewe, J., Stacke, T., Tessler, Z.D., Wada, Y., & Wisser, D. (2014). Global water resources affected by
627 human interventions and climate change. *Proceedings of the National Academy of Sciences of the United*
628 *States of America*, 111(9), 3251–6. doi:10.1073/pnas.1222475110

629 Hall, J., & Borgomeo, E. (2013). Risk-based principles for defining and managing water security Risk-based
630 principles for defining and managing water security. *Philosophical Transactions. Series A, Mathematical,*
631 *Physical, and Engineering Sciences*, 371(2002). <http://dx.doi.org/10.1098/rsta.2012.0407>

632 Hanasaki, N., Fujimori, S., Yamamoto, T., Yoshikawa, S., Masaki, Y., Hijioka, Y., Kainuma, M., Kanamori, Y.,
633 Masui, T., Takahashi, K., Kanae, S. (2013). A global water scarcity assessment under Shared Socio-
634 economic Pathways – Part 2: Water availability and scarcity. *Hydrology and Earth System Sciences*, 17,
635 2393–2413. doi:10.5194/hess-17-2393-2013

636 Hanemann, W. M. (2006). The economic conception of water. In *Water Crisis: myth or reality?* (pp. 61–90). Taylor
637 & Francis/Balkema, Leiden, The Netherlands

638 Hannah, D. M., Demuth, S., van Lanen, H. A. J., Looser, U., Prudhomme, C., Rees, G., Stahl, K., & Tallaksen, L.
639 M. (2011). Large-scale river flow archives: importance, current status and future needs. *Hydrological*
640 *Processes*, 25(7), 1191–1200. doi:10.1002/hyp.7794

641 Hoekstra, A.Y., Chapagain, A.K., Aldaya, M.M., Mekonnen, M.M. (2011). *Water footprint assessment manual:*
642 *Setting the global standard*. Earthscan, London, UK.

643 Hoekstra, A. Y., Mekonnen, M. M., Chapagain, A. K., Mathews, R. E., & Richter, B. D. (2012). Global monthly
644 water scarcity: blue water footprints versus blue water availability. *PloS One*, 7(2), e32688.
645 doi:10.1371/journal.pone.0032688

646 Howell, L. (2013). *Global Risks 2013*. World Economic Forum, Geneva, Switzerland

647 Hulme, M., Barrow, E. M., Arnell, N. W., Harrison, P. A., & Johns, T. C. (1999). Relative impacts of human-
648 induced climate change and natural climate variability. *Nature*, 397(6721), 688–691.

- 649 IPCC. (2013). Summary for Policymakers. Climate Change 2013: The Physical Science Basis. Contribution of
650 Working Group I to the Fifth Assessment Report of the Intergovernmental Panel on Climate Change.
651 Cambridge Univ. Press, Cambridge, UK.
- 652 Islam, Z., & Gan, T.Y. (2015) Future irrigation demand of South Saskatchewan river basin under the combined
653 impacts of climate change and El Nino Southern Oscillation. *Water Resour Manage*, 29, 2091-2105.
654 doi:10.1007/s11269-015-0930-1.
- 655 Kiem, A. S., & Franks, S. W. (2001). On the identification of ENSO-induced rainfall and runoff variability: a
656 comparison of methods and indices. *Hydrological Sciences Journal*, 46(5), 715–727.
657 doi:10.1080/02626660109492866
- 658 Kiguchi, M., Shen, Y., Kanae, S., & Oki, T. (2015). Reevaluation of future water stress due to socioeconomic and
659 climate factors under a warming climate. *Hydrological Sciences Journal*, 601(1), 14-29.
660 doi:10.1080/02626667.2014.888067
- 661 Kiladis, G. N., & Diaz, H. F. (1989). Global climatic anomalies associated with extremes in the Southern
662 Oscillation. *Journal of Climate*, 2, 1069–1090.
- 663 Klein Goldewijk, K., & van Drecht, G. (2006). HYDE 3: Current and historical population and land cover. MNP
664 (2006) (Edited by), In A. F. Bouwman, T. Kram, & K. Klein Goldewijk (Eds.), *Integrated modelling of*
665 *global environmental change. An overview of IMAGE 2.4.* Netherlands Environmental Assessment Agency
666 (MNP).
- 667 Kovats, R. S., Bouma, M. J., Hajat, S., Worrall, E., & Haines, A. (2003). El Niño and health. *The Lancet* 362(9394),
668 1481-1489. Doi: 10.1016/S0140-6736(03)14695-8
- 669 Kummu, M., Ward, P. J., de Moel, H., & Varis, O. (2010). Is physical water scarcity a new phenomenon? Global
670 assessment of water shortage over the last two millennia. *Environmental Research Letters*, 5(034006).
671 doi:10.1088/1748-9326/5/3/034006
- 672 Kummu, M., Gerten, D., Heinke, J., Konzmann, M., & Varis, O. (2014). Climate-driven interannual variability of
673 water scarcity in food production potential: a global analysis. *Hydrology and Earth System Sciences*, 18, 447–
674 461. doi:10.5194/hess-18-447-2014
- 675 Kundzewicz, Z. W., Mata, L. J., Arnell, N., Döll, P., Kabat, P., Jiménez, B., Miller, K., Oki, T., Şen, Z. &
676 Shiklomanov, I.(2007) Freshwater resources and their management. *Climate Change 2007: Impacts,*
677 *Adaptation and Vulnerability. Contribution of Working Group II to the Fourth Assessment Report of the*
678 *Intergovernmental Panel on Climate Change* (ed. by M. L. Parry, O. F. Canziani, J. P. Palutikof, P. J. van der
679 Linden & C. E. Hanson), 173–210. Cambridge University Press, UK. [http://www.ipcc.ch/pdf/assessment-](http://www.ipcc.ch/pdf/assessment-report/ar4/wg2/ar4-wg2-chapter3.pdf)
680 [report/ar4/wg2/ar4-wg2-chapter3.pdf](http://www.ipcc.ch/pdf/assessment-report/ar4/wg2/ar4-wg2-chapter3.pdf) [last accessed 8 January 2008].
- 681 Labat, D. (2010). Cross wavelet analyses of annual continental freshwater discharge and selected climate indices.
682 *Journal of Hydrology*, 385(1-4), 269–278. doi:10.1016/j.jhydrol.2010.02.029
- 683 Lehner, B., Döll, P., Alcamo, J., Henrichs, T., & Kaspar, F. (2006). Estimating the Impact of Global Change on
684 Flood and Drought Risks in Europe: A Continental, Integrated Analysis. *Climatic Change*, 75, 273–299.
685 doi:10.1007/s10584-006-6338-4
- 686 Livezey, R. E., & Chen, W. Y. (1982). Statistical field significance and its determination by monte carlo techniques.
687 *Monthly Weather Review*, 111, 46–59.

688 Lü, A., Jia, S., Zhu, W., Yan, H., Duan, S., & Yao, Z. (2011). El Niño-Southern Oscillation and water resources in
689 the headwaters region of the Yellow River: links and potential for forecasting. *Hydrology and Earth System*
690 *Sciences*, 15(4), 1273–1281. doi:10.5194/hess-15-1273-2011

691 Ludescher, J., Gozolchiani, A., Bogachev, M. I., Bunde, A., Havlin, S., & Schellnhuber, H. J. (2013). Correction for
692 Ludescher et al., Improved El Nino forecasting by cooperativity detection. *Proceedings of the National*
693 *Academy of Sciences of the United States of America*, 110(47), 19172–3. doi:10.1073/pnas.1317354110

694 Ludescher, J., Gozolchiani, A., Bogachev, M.I., Bunde, A., Havlin, S., Schellnhuber, H.J. (2014). Very early
695 warning of next El Niño. *Proc Natl Acad Sci USA* 111(6):2064–2066. doi: 10.1073/pnas.1323058111

696 Lundqvist, J., & Falkenmark, M. (2010). Adaptation to Rainfall Variability and Unpredictability: New Dimensions
697 of Old Challenges and Opportunities. *International Journal of Water Resources Development*, 26(4), 595–612.
698 doi:10.1080/07900627.2010.519488

699 McPhaden, M. J., Zebiak, S. E., & Glantz, M. H. (2006). ENSO as an integrating concept in earth science. *Science*,
700 314, 1740–1745. doi:10.1126/science.1132588

701 Meque, A., & Abiodun, B. J. (2014). Simulating the link between ENSO and summer drought in Southern Africa
702 using regional climate models. *Climate Dynamics*, 44(7-8), 1881–1900. doi:10.1007/s00382-014-2143-3

703 Meza, F.J. (2005) Variability of reference evapotranspiration and water demands. Association to ENSO in the
704 Maipo river basin, Chile. *Global and Planetary Change*, 47, 212–220. doi:10.1016/j.gloplacha.2004.10.013

705 Mosley, M. P. (2000). Regional differences in the effects of El Niño and La Niña on low flows and floods.
706 *Hydrological Sciences Journal*, 45(2), 249–267. doi:10.1080/02626660009492323

707 Moss, M. E., Pearson, C. P., & McKerchar, A. I. (1994). The Southern Oscillation index as a predictor of the
708 probability of low streamflows in New Zealand. *Water Resources Research*, 30, 2717–2723.

709 Müller Schmied, H., Eisner, S., Franz, D., Wattenbach, M., Portmann, F.T., Flörke, M., Döll, P. (2014) Sensitivity
710 of simulated global-scale freshwater fluxes and storages to input data, hydrological model structure, human
711 water use and calibration. *Hydrology and Earth System Sciences*, 18, 3511–3538. Doi:10.5194/hess-19-3511-
712 2014.

713 Murphy, J., Kattsov, V., Keenlyside, N., Kimoto, M., Meehl, G., Mehta, V., Pohlman, H., Scaife, A., & Smith, D.
714 (2010). Towards Prediction of Decadal Climate Variability and Change. *Procedia Environmental Sciences*, 1,
715 287–304. doi:10.1016/j.proenv.2010.09.018

716 Nazemi, A., & Wheeler, H. S. (2015a). On inclusion of water resource management in Earth System models – Part
717 1: Problem definition and representation of water demand. *Hydrology and Earth System Sciences*, 19, 33–61.
718 doi:10.5194/hess-19-33-2015

719 Nazemi, A., & Wheeler, H. S. (2015b). On inclusion of water resource management in Earth System models – Part
720 2: Representation of water supply and allocation and opportunities for improved modeling. *Hydrology and*
721 *Earth System Sciences*, 19, 63–90. doi:10.5194/hess-19-63-2015

722 Oki, T., Agata, Y., Kanae, S., Saruhashi, T., Yang, D., Musiak, K. (2001). Global assessment of current water
723 resources using total runoff integrating pathways. *Hydrological Sciences Journal*, 46, 983–995.
724 doi:10.1080/02626660109492890.

725 Oki, T., & Kanae, S. (2006). Global hydrological cycles and world water resources. *Science*, 313(5790), 1068–72.
726 doi:10.1126/science.1128845

727 Paeth, H., Scholten, A., Friederichs, P., Hense, A. (2008). Uncertainties in climate change prediction: El Niño
728 Southern Oscillation and monsoons. *Global Planet Change* 60(3-4), 265–288.
729 doi:10.1016/j.gloplacha.2007.03.002

730 Parker, D., Folland, C., Scaife, A., Knight, J., Colman, A., Baines, P., & Dong, B. (2007). Decadal to multidecadal
731 variability and the climate change background. *Journal of Geophysical Research: Atmospheres*, 112(D18).
732 Doi: <http://dx.doi.org/10.1029/2007JD008411>

733 Piechota, T. C., & Dracup, J. A. (1999). Long-range forecasting using El-Nino Southern Oscillations indicators.
734 *Journal Hydrological Engineering*, 4, 144–151.

735 Power, S., Delage, F., Chung, C., Kociuba, G., & Keay, K. (2013). Robust twenty-first-century projections of El
736 Niño and related precipitation variability. *Nature*, 502(7472), 541–5. doi:10.1038/nature12580

737 Prudhomme, C., Giuntoli, I., Robinson, E. L., Clark, D. B., Arnell, N. W., Dankers, R., Fekete, B.M., Franssen, W.,
738 Gerten, D., Gosling, S.N., Hagemann, S., Hannah, D.M., Kim, H., Masaki, Y., Satoh, Y., Stacke, T., Wada,
739 Y., & Wisser, D. (2014). Hydrological droughts in the 21st century, hotspots and uncertainties from a global
740 multimodel ensemble experiment. *Proceedings of the National Academy of Sciences of the United States of*
741 *America*, 111(9), 3262–7. doi:10.1073/pnas.1222473110

742 Räsänen, T. A., & Kumm, M. (2013). Spatiotemporal influences of ENSO on precipitation and flood pulse in the
743 Mekong River Basin. *Journal of Hydrology*, 476, 154–168. doi:10.1016/j.jhydrol.2012.10.028

744 Raskin, P., P. Gleick, P. Kirshen, G. Pontius, and K. Strzepek. (1997). *Water Futures: Assessment of long-range*
745 *patterns and problems. Comprehensive assessment of the freshwater resources of the world.* Stockholm
746 Environment Institute, Box 2142. S-103 14, Stockholm, Sweden.

747 Richard, Y., Fauchereau, N., Pocard, I., Rouault, M., & Trzaska, S. (2001). 20th century droughts in southern
748 africa: spatial and temporal variability, teleconnections with oceanic and atmospheric conditions. *International*
749 *Journal of Climatology*, 21(7), 873–885. doi:10.1002/joc.656

750 Richter, B.D., Davis, M.M., Apse, C., Konrad, C. (2011). A presumptive standard for environmental flow
751 protection. *River Res Appl.* 28(8), 1312-1321. doi:10.1002/rra.1511.

752 Rijsberman, F. (2006). Water scarcity: Fact or fiction? *Agricultural Water Management*, 80, 5–22.
753 doi:10.1016/j.agwat.2005.07.001

754 Ropelewski, C.F., & Halpert, M.S. (1987). Global and regional scale precipitation patterns associated with the El
755 Nino/Southern Oscillation. *Monthly Weather Review*, 115, 1606-1626.

756 Rosegrant, M. W., Cai, X. M., & Cline, S. (2002). *World water and food to 2025. Dealing with scarcity.*
757 International Food Policy Research Institute, Washington, D.C.

758 Rosenzweig, C., & Hillel, D. (2008). Climate variability and the global harvest: Impacts of El Nino and other
759 oscillations on agro-ecosystems (p. 280). Oxford University Press, New York.

760 Savenije, H.H.G. (2000). Water scarcity indicators; the deception of the numbers. *Phys. Chem. Earth (B)*, 25(3),
761 199-204. Doi: 10.1016/S1464-1909(00)00004-6.

762 Schewe, J., Heinke, J., Gerten, D., Haddeland, I., Arnell, N. W., Clark, D. B., Dankers, R., Eisner, S., Fekete, B.M.,
763 Colón-González, F.J., Gossling, S.N., Kim, H., Liu, X., Masaki, Y., Portmann, F.T., Satoh, Y., Stacke, T.,
764 Tang, Q., Wada, Y., Wisser, D., Albrecht, T., Frieler, K., Piontek, F., Warszawski, L., & Kabat, P. (2014).
765 Multimodel assessment of water scarcity under climate change. *Proceedings of the National Academy of*
766 *Sciences of the United States of America*, 111(9), 3245–3250. doi:10.1073/pnas.1222460110

767 Schmidt, N., Lipp, E. K., Rose, J. B., & Luther, M. E. (2001). ENSO Influences on Seasonal Rainfall and River
768 Discharge in Florida. *Journal of Climate*, 14, 615 – 628. doi: [http://dx.doi.org/10.1175/1520-](http://dx.doi.org/10.1175/1520-0442(2001)014<0615:EIOSRA>2.0.CO;2)
769 [0442\(2001\)014<0615:EIOSRA>2.0.CO;2](http://dx.doi.org/10.1175/1520-0442(2001)014<0615:EIOSRA>2.0.CO;2)

770 Seneviratne, S.I., Koster, R.D., Guo, Z., Dirmeyer, P.A., Kowalczyk, E., Lawrence, D., Liu, P., Lu, C.-H., Mocko,
771 D., Oleson, K.W., Verseghy, D. (2006). Soil moisture memory in AGCM simulations: Analysis of global
772 land-atmosphere coupling experiment (GLACE) data. *Journal of hydrometeorology*, 7(5), 1090-1112. Doi:
773 <http://dx.doi.org/10.1175/JHM533.1>.

774 Sharma, A. (2000). Seasonal to interannual rainfall probabilistic forecasts for improved water supply management :
775 Part 3 — A nonparametric probabilistic forecast model. *Journal of Hydrology*, 239(1-4), 249–258.
776 doi:10.1016/S0022-1694(00)00348-6

777 Sheffield, J., Andreadis, K.M., Wood, E.F., Lettenmaier, D.P. (2008) Global and Continental Drought in the Second
778 Half of the Twentieth Century: Severity-Area-Duration Analysis and Temporal Variability of Large-Scale
779 Events. *Journal of Climate*, 22, 1962-1981. doi: 10.1175/2008JCLI2722.1

780 Smit, B., Pilifosova, O. (2003). From adaptation to adaptive capacity and vulnerability reduction. In: Smith, J.B.,
781 Klein, R.J.T., Huq, S. (Eds.), *Climate Change, Adaptive Capacity and Development*. Imperial College Press,
782 London.

783 Sperna Weiland, F. C., van Beek, L. P. H., Kwadijk, J. C. J., & Bierkens, M. F. P. (2012). Global patterns of change
784 in discharge regimes for 2100. *Hydrology and Earth System Sciences*, 16, 1047–1062. doi:10.5194/hess-16-
785 1047-2012

786 Stahl, K. (2001). Hydrological Drought - a Study across Europe. PhD Thesis. *Freiburger Schriften zur hydrologie*
787 (No. 15). Institut für Hydrologie, Universität Freiburg, Freiburg.

788 Suarez, P., Hansen, J. W., Carriquiry, M., Mishra, A. K., & Osgood, D. (2008). Integrating seasonal forecasts and
789 insurance for adaptation among subsistence farmers: The case of Malawi (No. 4651). *World Bank Policy*
790 *Research Working Paper series*, available at SSRN: <http://ssrn.com/abstract=1149603>, last access: 5 May
791 2015.

792 Van Beek, L. P. H., Wada, Y., & Bierkens, M. F. P. (2011). Global monthly water stress: 1. Water balance and
793 water availability. *Water Resources Research*, 47, W07517. doi:10.1029/2010WR009791

794 Van Oldenborgh, G.J., Philip, S.Y., Collins, M. (2005) El Niño in a changing climate: A multimodel study. *Ocean Sci*
795 1:81–95. doi:10.5194/os-1-81-2005

796 Van Vliet, M. T. H., Franssen, W. H. P., Yearsley, J. R., Ludwig, F., Haddeland, I., Lettenmaier, D. P., & Kabat, P.
797 (2013). Global river discharge and water temperature under climate change. *Global Environmental Change*,
798 23(2), 450–464. doi:10.1016/j.gloenvcha.2012.11.002

799 Veldkamp, T. I. E., Wada, Y., de Moel, H., Kummerow, M., Eisner, S., Aerts, J. C. J. H., & Ward, P. J. (2015).
800 Changing mechanism of global water scarcity events: Impacts of socioeconomic changes and inter-annual
801 hydro-climatic variability. *Global Environmental Change*, 32, 18–29. doi:10.1016/j.gloenvcha.2015.02.011

802 Vicente-Serrano, S.M., Lopez-Moreno, J.I., Gimeno, L., Nieto, R., Moran-Tejeda, E., Lorenzo-Lacruz, J., Begueria,
803 S., Azorin-Molina, C. (2011) A multiscalar global evaluation of the impacts of ENSO on droughts. *Journal of*
804 *Geophysical Research*, 116, D20109. doi:10.1029/2011JD016039.

805 Vörösmarty, C. J., Green, P., Salisbury, J., & Lammers, R. B. (2000). Global Water Resources: Vulnerability from
806 Climate Change and Population Growth. *Science*, 289, 284–288. doi:10.1126/science.289.5477.284

807 Wada, Y., van Beek, L. P. H., & Bierkens, M. F. P. (2011a). Modelling global water stress of the recent past: on the
808 relative importance of trends in water demand and climate variability. *Hydrology and Earth System Sciences*,
809 15, 3785–3808. doi:10.5194/hess-15-3785-2011

810 Wada, Y., van Beek, L. P. H., Viroli, D., Dürr, H. H., Weingartner, R., & Bierkens, M. F. P. (2011b). Global
811 monthly water stress: 2. Water demand and severity of water stress. *Water Resources Research*, 47, W07518.
812 doi:10.1029/2010WR009792

813 Wada, Y., Gleeson, T., & Esnault, L. (2014a). Water wedges : regional strategies to global water resource Wedge
814 approach to water stress, *Nat. Geosci.*, 7, 615–617. doi:10.1038/NGEO2241

815 Wada, Y., Wisser, D., & Bierkens, M. F. P. (2014b). Global modeling of withdrawal, allocation and consumptive
816 use of surface water and groundwater resources. *Earth System Dynamics*, 5(1), 15–40. doi:10.5194/esd-5-15-
817 2014

818 Wallace, J. M., & Hobbs, P. (2006). *Atmospheric Science* (2nd edition., p. 504). Academic Press.

819 Wang, C., Xie, S., & Carton, J. A. (2004). A Global Survey of Ocean – Atmosphere Interaction and Climate
820 Variability. In *Earth Climate: The Ocean-Atmospheric Interaction* (pp. 1–19). American Geophysical Union,
821 Washington, D.C., 1–19, doi:10.1029/147GM01, 2004.

822 Ward, P. J., Aerts, J. C. J. H., de Moel, H., & Renssen, H. (2007). Verification of a coupled climate-hydrological
823 model against Holocene palaeohydrological records. *Global and Planetary Change*, 57, 283–300.
824 doi:10.1016/j.gloplacha.2006.12.002

825 Ward, P. J., Beets, W., Bouwer, L. M., Aerts, J. C. J. H., & Renssen, H. (2010). Sensitivity of river discharge to
826 ENSO. *Geophysical Research Letters*, 37(12), L12402. doi:10.1029/2010GL043215

827 Ward, P. J., Eisner, S., Flörke, M., Dettinger, M. D., & Kummerow, M. (2014a). Annual flood sensitivities to El Niño–
828 Southern Oscillation at the global scale. *Hydrology and Earth System Sciences*, 18(1), 47–66.
829 doi:10.5194/hess-18-47-2014

830 Ward, P. J., Jongman, B., Kummerow, M., Dettinger, M. D., Sperna Weiland, F. C., & Winsemius, H. C. (2014b).
831 Strong influence of El Niño Southern Oscillation on flood risk around the world. *Proceedings of the National*
832 *Academy of Sciences*, 1–6. doi:10.1073/pnas.1409822111

833 Weedon, G. P., Gomes, S., Viterbo, P., Shuttleworth, W. J., Blyth, E., Österle, H., Adam, J. C., Bellouin, N.,
834 Boucher, O., & Best, M. (2011). Creation of the watch forcing data and its use to assess global and regional
835 reference crop evaporation over land during the twentieth century. *J. Hydrometeorol*, 12, 823–848. doi:
836 <http://dx.doi.org/10.1175/2011JHM1369.1>

837 Weedon, G.P., Balsamo, G., Bellouin, N., Gomes, S., Best, M.J., & Viterbo, P. (2014). The WFDEI meteorological
838 forcing data set: WATCH Forcing Data methodology applied to ERA-Interim reanalysis data. *Water*
839 *Resources Research*, 50, 7505-7514. doi: <http://dx.doi.org/10.1002/2014WR015638>

- 840 Whetton, P. H., Adamson, D. A., & Wilson, M. A. J. (1990). Rainfall and river flow variability in Africa, Australia
841 and East Asia linked to El Nino –Southern Oscillation events, in: Lessons for Human Survival: Nature’s
842 record from the Quaternary, edited by: Bishop, P., Geological Society of Australia Symposium Proceedings, 1,
843 71–82, 1990.
- 844 Wilks, D.S. (2006) On ‘Field significance’ and the false discovery rate. *Journal of Applied meteorology and*
845 *climatology*, vol. 45, 1181-1189. <http://dx.doi.org/10.1175/JAM2404.1>
- 846 Young, R. A. (2005). Determining the economic value of water: Concepts and methods, *Resources for the Future* (p.
847 357). Washington D.C., USA
- 848 Zebiak, S. E., Orlove, B., Muñoz, Á. G., Vaughan, C., Hansen, J., Troy, T., Thomson, M.C., Lustig, A., & Garvin,
849 S. (2014). Investigating El Niño-Southern Oscillation and society relationships. *Wiley Interdisciplinary*
850 *Reviews: Climate Change*, 6, 17–34, doi:10.1002/wcc.294.

Tables

Table 1. Hydrological years that fall under the El Niño and La Niña phase. Other years are classified as ENSO neutral.

ENSO phase	Hydrological year
El Niño	1964,1966,1970, 1973, 1977,1983,1987,1988,1992,1998, 2003, 2007, 2010
La Niña	1965,1968,1971,1972,1974,1975,1976,1989,1999,2000,2008

Table 2. Percentage of the global land area for which (a) water resources availability and (b) consumptive water use show a significant (positive/negative) correlation with ENSO driven climate variability (as assessed with the JMA SST anomaly index).

	Significant correlation	Sign. positive correlation	Sign. negative correlation
Water Availability	37.1 %	13.2 %	23.9 %
Consumptive water use	8.3 %	1.0 %	7.3 %

Table 3. Percentage of the global land area for which water scarcity conditions show a significant (positive/negative) correlation with ENSO driven climate variability (as assessed with the JMA SST anomaly index). Water scarcity conditions were assessed by means of the CTA-ratio for water stress and WCI-ratio for water shortage.

	Significant correlation	Sign. positive correlation	Sign. negative correlation
Consumption to Availability Ratio (CTA-ratio)	28.1 %	16.8 %	11.3 %
Water Crowding Index (WCI)	37.9 %	23.9 %	14.0 %

Table 4. Percentage of the global land area for which FPU's show significant anomalies in the median values of water scarcity conditions between the El Niño (EN) and La Niña (LN) phase, compared to the median values under all years. Water scarcity conditions were assessed by means of the CTA-ratio for water stress and WCI-ratio for water shortage.

	Significant Anomaly	Sign. Anomaly – El Nino Phase	Sign. Anomaly – La Nina Phase
Consumption to Availability Ratio (CTA-ratio)	12.8 %	3.4 %	12.8 %
Water Crowding Index WCI)	14.8 %	6.9 %	9.5 %

Table 5. Development of (a) the global total population, (b) the global population exposed to water scarcity events (CTA-ratio), (c) the global population living in areas sensitive to ENSO driven climate variability, and (d) the global population being exposed to water scarcity events (CTA-ratio) & living in areas sensitive to ENSO driven climate variability, between 1961 and 2010 using 5-year averaged values. Numbers between brackets show the values expressed in percentage of the total population. Growth factors represent both the absolute increases as well as the relative increases over time.

	Total Population	Population exposed to water scarcity events(CTA ≥ 0.2)	Population sensitive to ENSO driven climate-variability	Population sensitive to ENSO driven climate-variability & exposed to water scarcity events (CTA ≥ 0.2)
1961-1965	2.97 billion	0.45 billion (15.3%)	0.85 billion (28.7%)	0.2 billion (6.8%)
2006-2010	6.25 billion	2.48 billion (39.6%)	1.96 billion (31.3%)	0.71 billion (11.4%)
Growth factor	2.1	5.5 (2.6)	2.3 (0.4)	3.5 (1.5)

Table A. 1. Development of (a) the global total population, (b) the global population exposed to water scarcity events (WCI), (c) the global population living in areas sensitive to ENSO driven climate variability, and (d) the global population being exposed to water scarcity events (WCI) & living in areas sensitive to ENSO driven climate variability, between 1961 and 2010 using 5-year averaged values. Numbers between brackets show the values expressed in percentage of the total population. Growth factors represent both the absolute increases as well as the relative increases over time.

	Total Population	Population exposed to water scarcity events(WCI≤1700)	Population sensitive to ENSO driven climate-variability	Population sensitive to ENSO driven climate-variability & exposed to water scarcity events (WCI≤1700)
1961-1965	2.97 billion	0.39 billion (13.2%)	1.01 billion (34.1%)	0.14 billion (4.8%)
2006-2010	6.25 billion	2.57 billion (41.1%)	2.41 billion (38.6%)	0.99 billion (15.9%)
Growth factor	2.1	6.6 (3.1)	2.4 (0.4)	6.9 (2.9)

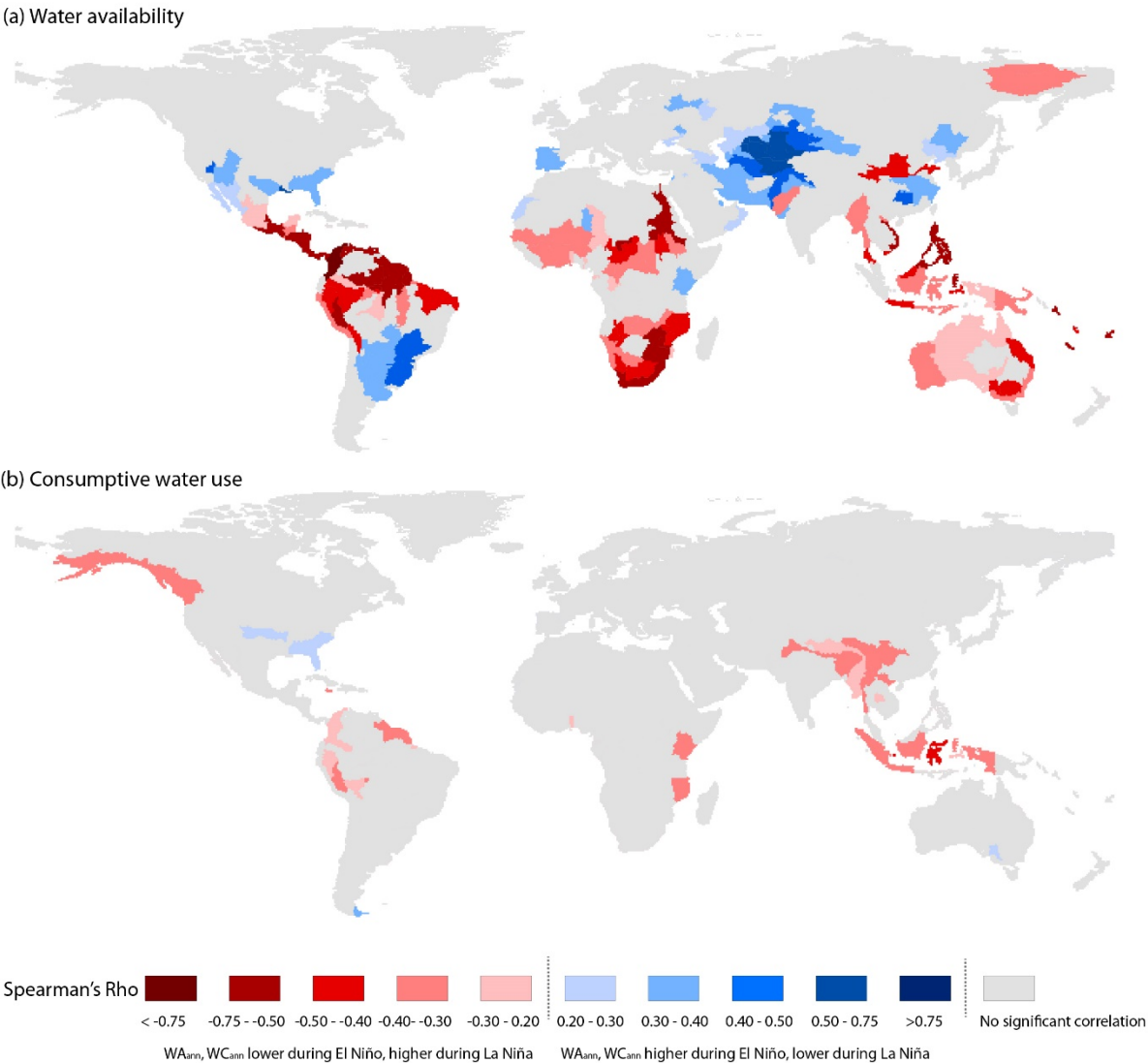


Figure 1. Correlation (Spearman's Rho) of yearly (a) water availability and (b) consumptive water use values, as assessed under fixed socioeconomic conditions, to variations in JMA SST using the 3-monthly period with the highest correlation (JMA SST_{bestoff}). Significance was tested by means of regular bootstrapping (n = 1000, p ≤ 0.05) and the correlation is only shown for those areas which reach significance. Positive correlations indicate increases in annual water availability and consumption with the JMA SST_{bestoff} index moving towards El Niño values. Negative correlations indicate decreases in annual water availability with the JMA SST_{bestoff} index moving towards El Niño values.

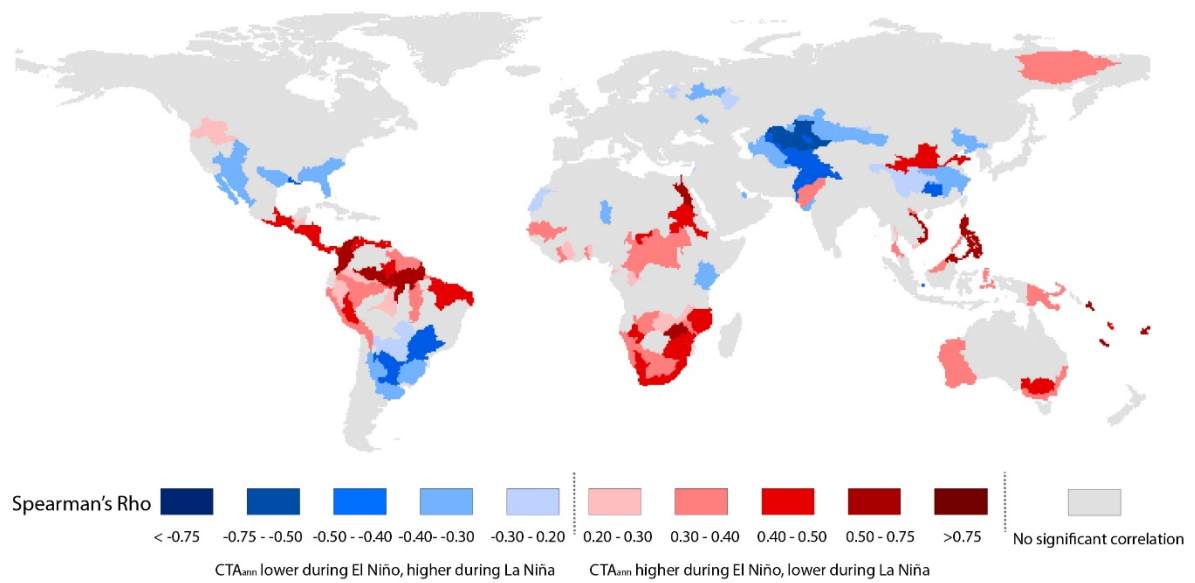


Figure 2. Correlation (Spearman's Rho) of yearly water scarcity conditions (CTA-ratio), as assessed under fixed socioeconomic conditions, to variations in JMA SST using the 3-monthly period with the highest correlation (JMA SST_{bestoff}). Significance was tested by regular bootstrapping ($n = 1000$, $p \leq 0.05$) and the correlation is only shown for those areas with significant correlations. Positive correlations indicate increases in CTA-ratio values (more severe water scarcity conditions) with the JMA SST_{bestoff} index moving towards El Niño values. Negative correlations indicate decreases in CTA-ratio values (less severe water scarcity conditions) with the JMA SST_{bestoff} index moving towards El Niño values.

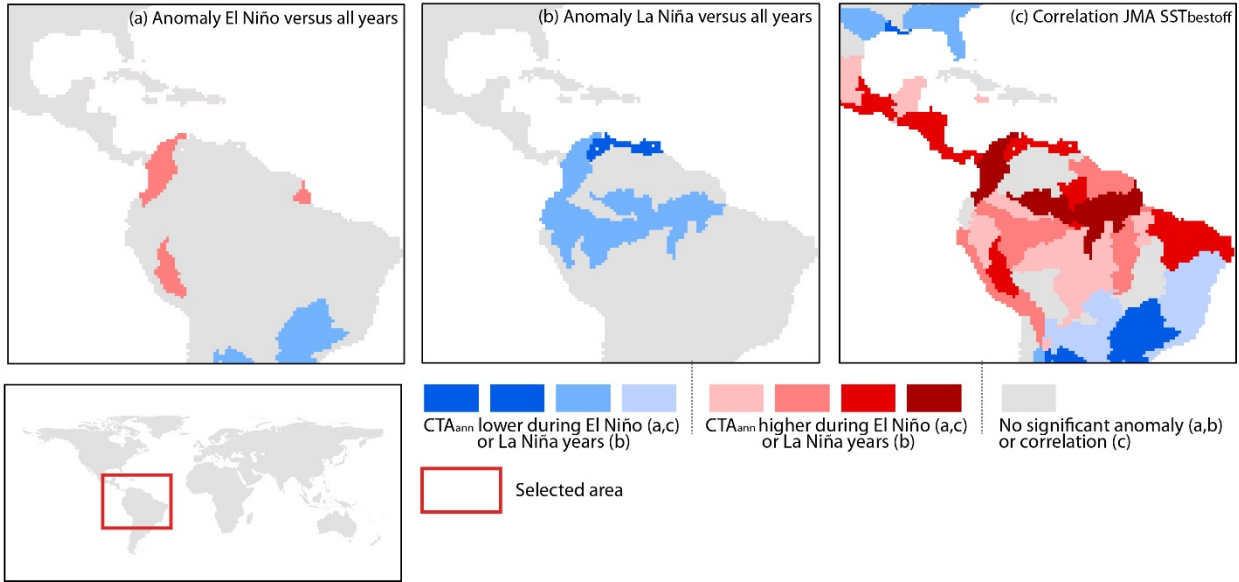


Figure 3. Comparison of results found when studying the: (a) anomaly in water scarcity conditions (CTA-ratio) between El Niño and all years; (b) anomaly in water scarcity conditions (CTA-ratio) between La Niña and all years; and (c) the sensitivity of water scarcity conditions (CTA-ratio) to ENSO driven climate variability measured by means of the JMA SST_{bestoff}. Red colors indicate more severe scarcity conditions under El Niño phases (a,c) or La Niña phases (b). Blue colors indicate less severe scarcity conditions under El Niño phases (a,c) or La Niña phases (b).

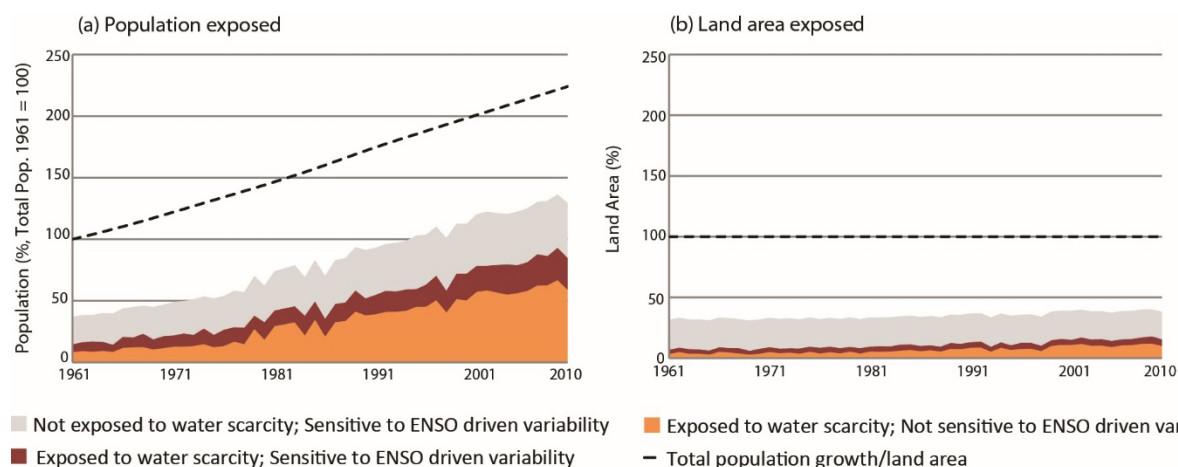


Figure 4. Development of population and land-area exposed to water scarcity events and/or being sensitive to ENSO driven climate variability over the period 1961-2010, as estimated with the CTA-ratio. Figure 4.A shows the growth in population living under water scarce conditions and/or living in areas sensitive to ENSO driven climate variability relative to the total growth in global population (set at 100 in 1961). Figure 4.B shows the increase in land-area exposed to either water scarcity events and/or ENSO driven climate variability relative to the total global land-area (100).

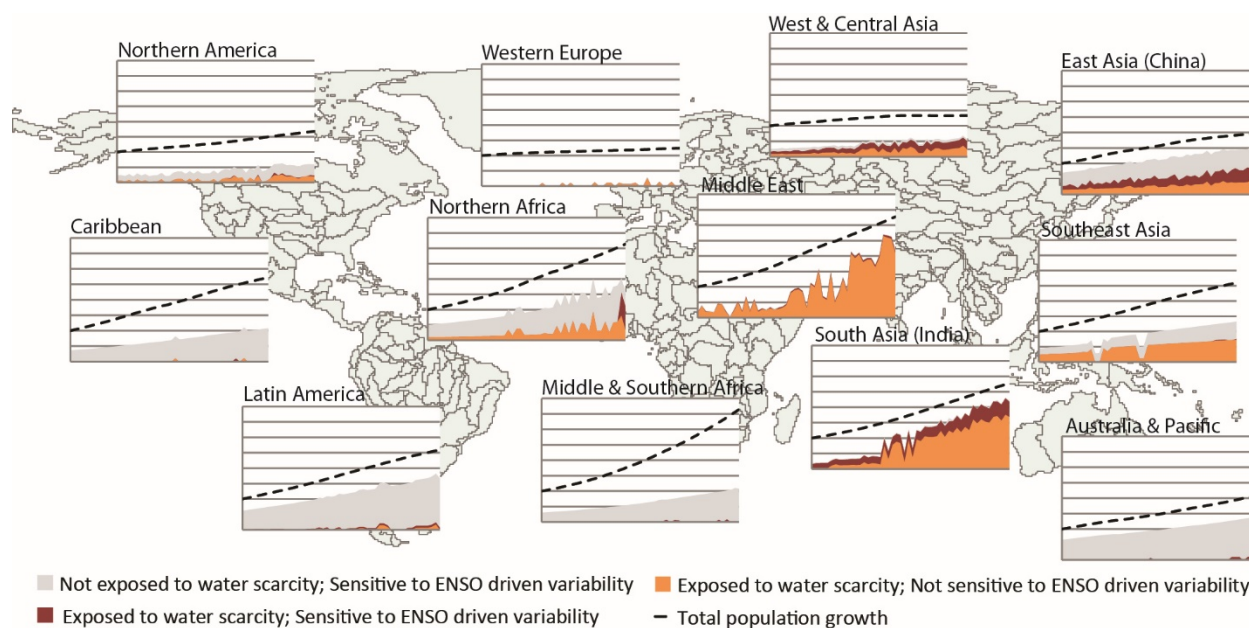


Figure 5. Regional variation in developments of population (%) exposed to water scarcity events and/or being sensitive to ENSO driven climate variability over the period 1961-2010, as estimated with the CTA-ratio. The figure shows per world region the growth in population living under water scarcity conditions and/or living in areas sensitive to ENSO driven climate variability, relative to the total growth in global population (set at 100 in 1961). Y-axis (% population) ranges from 0 up to 400.

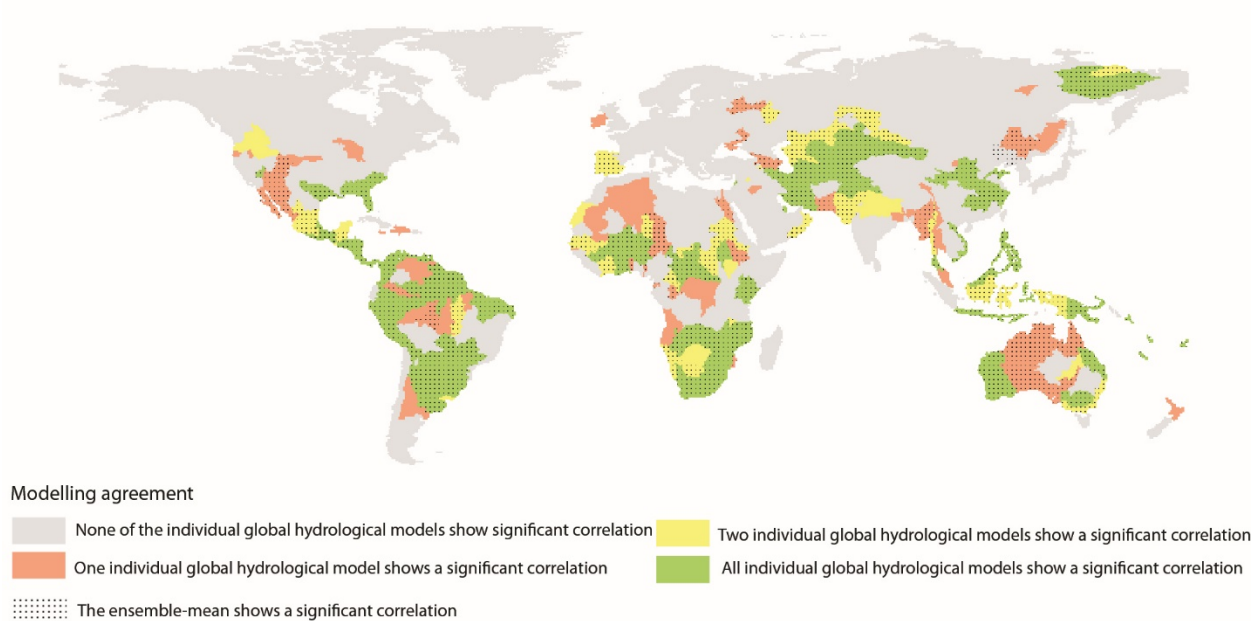
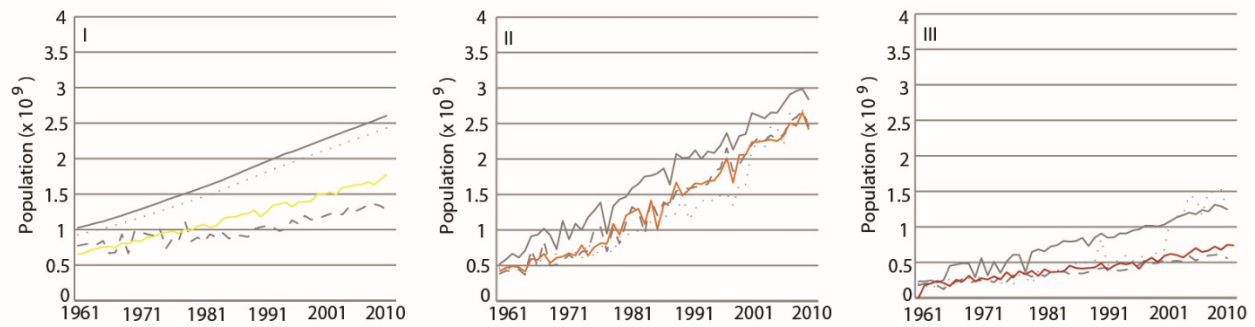


Figure 6. Modelling agreement in observed significant sensitivity of water availability to variation in JMA SST.

(a) Consumption To Availability Ratio



(b) Water Crowding Index

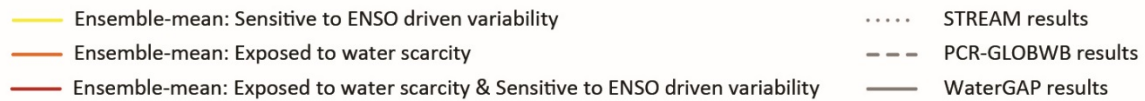
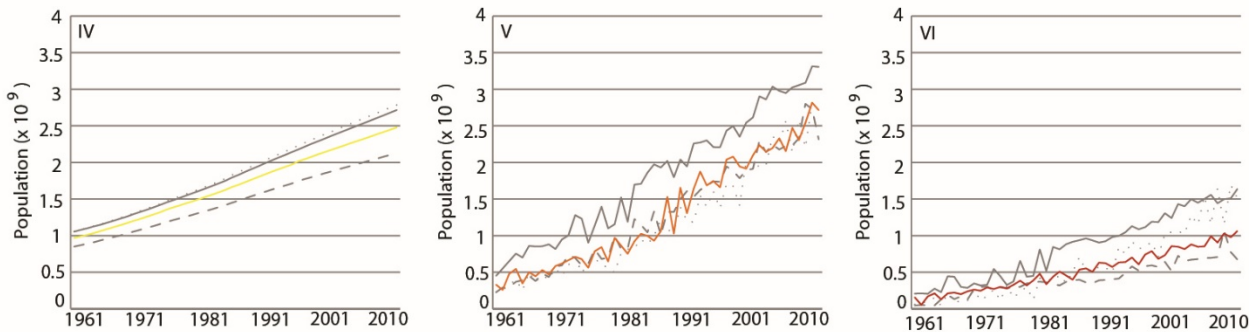


Figure 7. Development of the population and land-area exposed to water scarcity events (CTA-ratio) and/or being sensitive to ENSO driven climate variability over the period 1961-2010, as assessed by the individual global hydrological models (STREAM, PCR-GLOBWB, and WaterGAP) and the ensemble-mean. Fig. I and IV show the development in population sensitive to ENSO driven climate variability as estimated under the ensemble-mean (yellow) and individual GHMs (grey). Fig. II and V present the increase in population exposed to water scarcity events for the ensemble-mean (orange) and individuals GHMs (grey). Fig. III and VI visualize the amount of people being exposed to water scarcity events while at the same time living in areas with a significant correlation to ENSO driven climate variability for the ensemble-mean (red) and individual GHMs (red).

Appendix A: Supplementary Figures

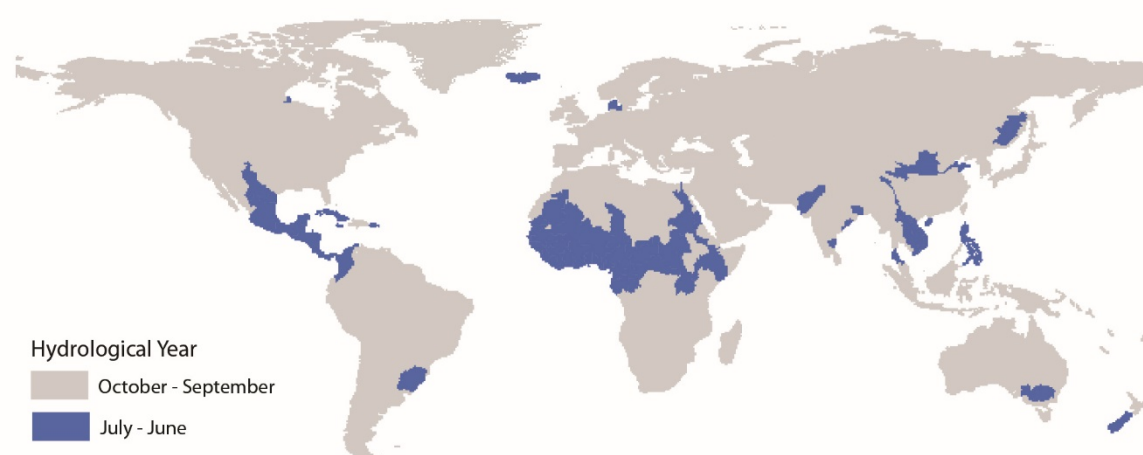


Fig. A 1. Hydrological years used in this study.

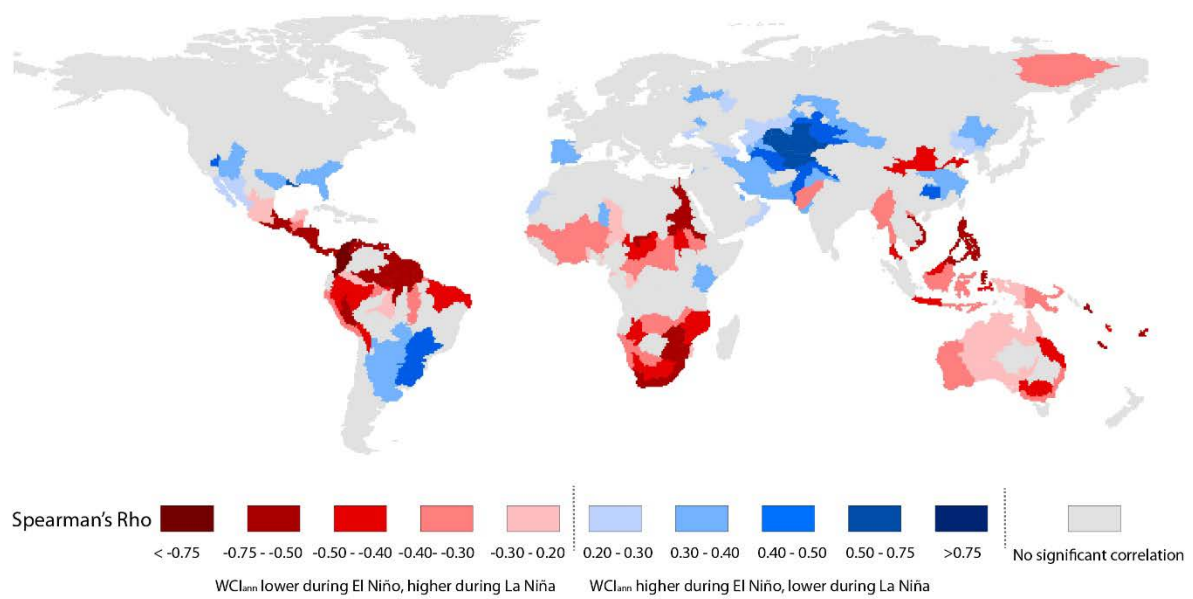


Fig. A 2. Correlation (Spearman's Rho) of yearly water scarcity conditions (WCI), as assessed under fixed socioeconomic conditions, to variations in JMA SST using the 3-monthly period with the highest correlation (JMA SST_{bestoff}). Significance was tested by regular bootstrapping ($n = 1000$, $p \leq 0.05$) and the correlation is only shown for those areas with significant correlations. Positive correlations indicate increases in WCI values (less severe water scarcity conditions) with the JMA SST_{bestoff} index moving towards El Niño values. Negative correlations indicate decreases in WCI values (more severe water scarcity conditions) with the JMA SST_{bestoff} index moving towards El Niño values.

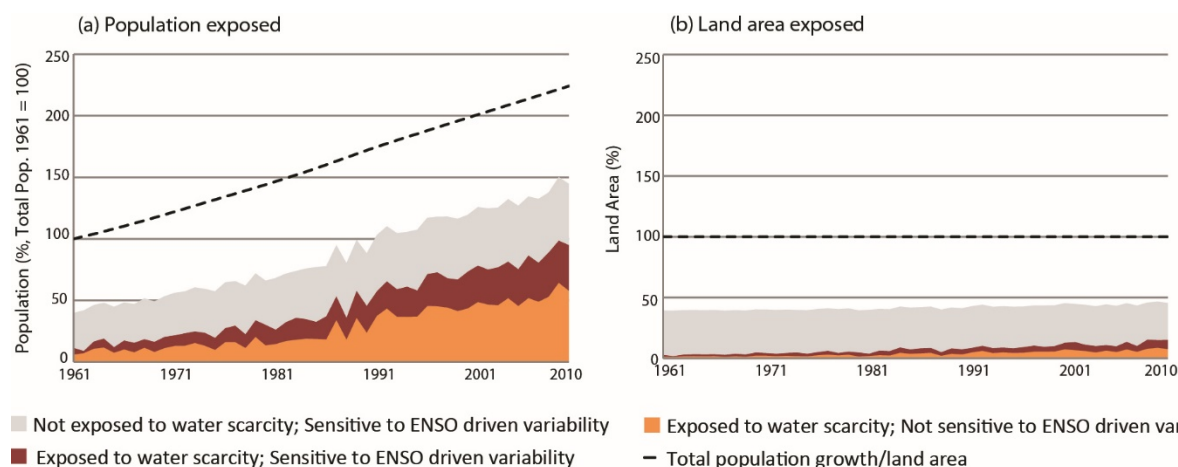


Fig. A 3. Development of population and land-area exposed to water scarcity events and/or being sensitive to ENSO driven climate variability over the period 1961-2010, as estimated with the WCI. Figure A.3.A shows the growth in population living under water scarce conditions and/or living in areas sensitive to ENSO driven climate variability relative to the total growth in global population (set at 100 in 1961). Figure A.3.B shows the increase in land-area exposed to either water scarcity events and/or ENSO driven climate variability relative to the total global land-area (100).

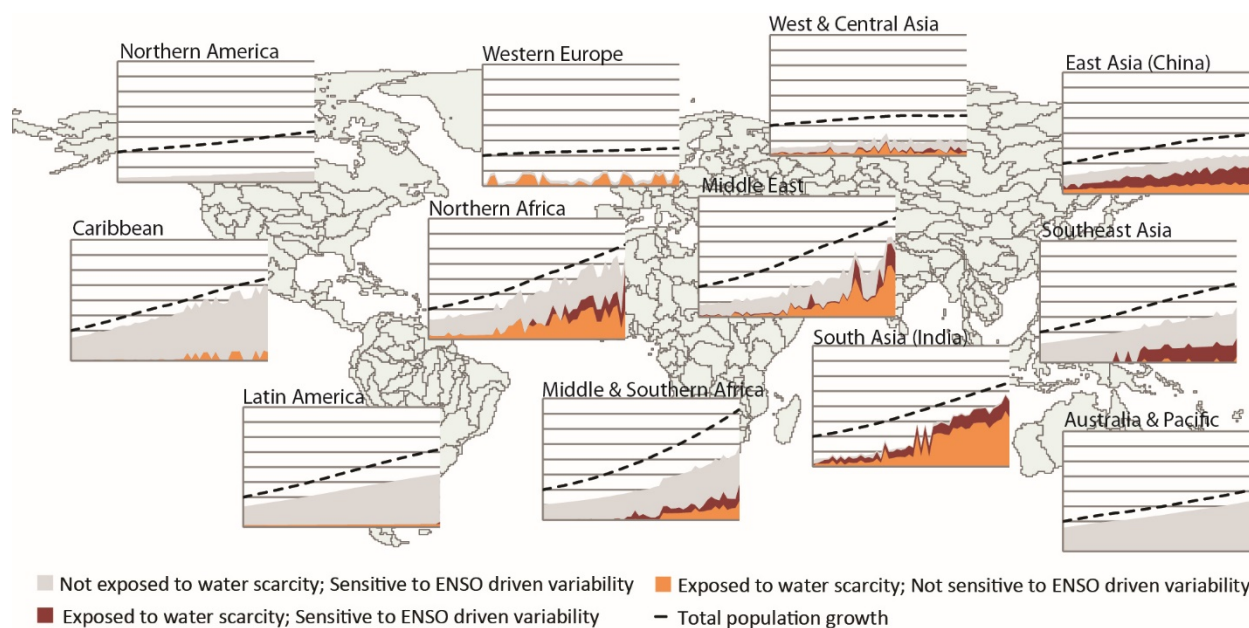
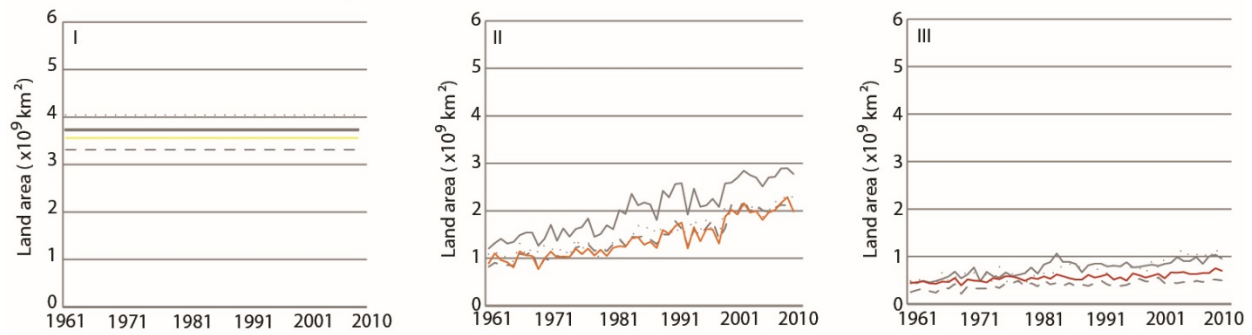


Fig. A 4. Regional variation in developments of population (%) exposed to water scarcity events and/or being sensitive to ENSO driven climate variability over the period 1961-2010, as estimated with the WCI. The figure shows per world region the growth in population living under water scarcity conditions and/or living in areas sensitive to ENSO driven climate variability, relative to the total growth in global population (set at 100 in 1961). Y-axis (% population) ranges from 0 up to 400

(a) Consumption To Availability Ratio



(b) Water Crowding Index

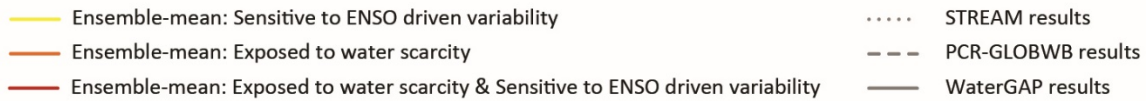
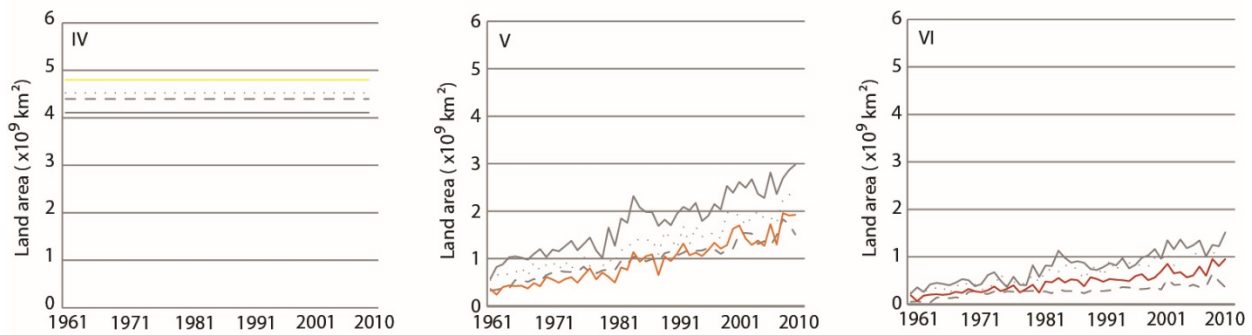


Fig. A 5. Development of the population and land-area exposed to water scarcity events (WCI) and/or being sensitive to ENSO driven climate variability over the period 1961-2010, as assessed by the individual global hydrological models (STREAM, PCR-GLOBWB, and WaterGAP) and the ensemble-mean. Fig. I and IV show the development in population sensitive to ENSO driven climate variability as estimated under the ensemble-mean (yellow) and individual GHMs (grey). Fig. II and V present the increase in population exposed to water scarcity events for the ensemble-mean (orange) and individuals GHMs (grey). Fig. III and VI visualize the amount of people being exposed to water scarcity events while at the same time living in areas with a significant correlation to ENSO driven climate variability for the ensemble-mean (red) and individual GHMs (red).